CALIFORNIA ENERGY COMMISSION

Energy Research and Development Division

FINAL PROJECT REPORT

Development, Implementation, and Integration of a Holistic Solar Forecasting System for California

May 2023 | CEC-500-2023-025

PREPARED BY:

Primary Authors:
Qin Wang Phone: (650) 855-8570
Aidan Tuohy Phone: (865) 387-5298
Naresh Kumar Phone: (650) 855-8758
Ben Kaldunski Phone: (650) 855-8526
Electric Power Research Institute (EPRI)
3420 Hillview Avenue, Palo Alto, CA 94304
Phone: (650) 855-8570
https://www.epri.com

Kenneth Craig
Sonoma Technology, Inc.
1450 N. McDowell Blvd., Suite 200, Petaluma, CA 94954
Phone: 707-665-9900
http://www.sonomatech.com/

Daniel Kirk-Davidoff
UL Renewables/AWS Truepower
463 New Karner Road, Albany, NY 12205
Phone: 518-213-0044
https://www.aws-dewi.ul.com

Contract Number: EPC-17-006

PREPARED FOR:
California Energy Commission

Silvia Palma-Rojas
Project Manager

Kevin Uy
Office Manager
ENERGY GENERATION RESEARCH OFFICE

Jonah Steinbuck, Ph.D.
Deputy Director
ENERGY RESEARCH AND DEVELOPMENT DIVISION

Drew Bohan
Executive Director

DISCLAIMER

ACKNOWLEDGEMENTS

Qin Wang, Aidan Tuohy, Naresh Kumar, and Ben Kaldunski from the Electric Power Research Institute (EPRI) served as the primary project managers for this work. EPRI also provided supplemental funding for research activities conducted during the course of this project with significant contributions from EPRI staff Qin Wang and Aidan Tuohy. Daniel Kirk-Davidoff (UL Renewables/AWS Truepower) and Kenneth Craig (STI) provided valuable contributions, insight and feedback on data collection/acquisition, analysis, and development of the real-time data website. The research team is grateful for the engagement and feedback provided by the technical advisory committee members whose input has been incorporated into this report. The research team is grateful to the California Energy Commission for providing funding through the EPIC program to support this important research project.

PREFACE

The California Energy Commission's (CEC) Energy Research and Development Division supports energy research and development programs to spur innovation in energy efficiency, renewable energy and advanced clean generation, energy-related environmental protection, energy transmission, and distribution and transportation.

In 2012, the Electric Program Investment Charge (EPIC) was established by the California Public Utilities Commission (CPUC) to fund public investments in research to create and advance new energy solutions, foster regional innovation, and bring ideas from the lab to the marketplace. The CEC and the state's three largest investor-owned utilities—Pacific Gas and Electric Company, San Diego Gas & Electric Company, and Southern California Edison Company—were selected to administer the EPIC funds and advance novel technologies, tools, and strategies that provide benefits to their electric ratepayers.

The CEC is committed to ensuring public participation in its research and development programs that promote greater reliability, lower costs, and increase safety for the California electric ratepayer and include:

- Providing societal benefits.
- Reducing greenhouse gas emission in the electricity sector at the lowest possible cost.
- Supporting California's loading order to meet energy needs first with energy efficiency and demand response, next with renewable energy (distributed generation and utility scale), and finally with clean, conventional electricity supply.
- Supporting low-emission vehicles and transportation.
- Providing economic development.
- Using ratepayer funds efficiently.

Development, Implementation, and Integration of a Holistic Solar Forecasting System for California is the final report for the project with the same name (contract number EPC-17-006 under GFO-16-309) conducted by Electric Power Research Institute. The information from this project contributes to the Energy Research and Development Division's EPIC Program.

For more information about the Energy Research and Development Division, please visit the CEC's research website (www.energy.ca.gov/research/) or contact the CEC at 916-327-1551.

ABSTRACT

Errors in forecasting the development and breakup of fog and low coastal clouds are an important contributor to errors in forecasts of California's solar generation. To improve solar generation forecasting capabilities, this project set up and performed a series of experiments using the Weather Research and Forecasting numerical weather prediction model. These experiments tested the sensitivity of the model's ability to forecast foggy conditions using a range of parameterization choices. A measurement program involving targeted use of ground-based atmospheric boundary layer sensors was successfully completed from December 2017 through March 2019 to support improvements in predicting fog and stratus cloud (low level cloud) dissipation in high solar penetration regions of California.

Analysis of power grid operating data showed no simple correlation between solar forecasting errors and electric grid operation metrics. Production cost modeling simulation analysis showed that with 20 percent solar forecast accuracy improvement in day-ahead forecasting, the fuel cost and startup cost of thermal units in the system could be reduced by between 0.06 percent and 3 percent, depending on test systems. These results can help to guide users and producers of solar generation forecasts towards prioritizing and properly valuing improved forecasting technologies. Finally, the impacts of improved solar power forecasting and battery storage resources to the system were compared. In the modified California system, the economic value of 20 percent solar power forecasting improvement is similar to that of a 25 MW battery storage resource.

Keywords: solar generation forecast, data assimilation, remote sensing, numerical weather prediction, coastal stratus, fog, WRF, machine learning, value, benefits

Please use the following citation for this report:

Qin Wang, Kenneth Craig, Daniel Kirk-Davidoff, Aidan Tuohy, Naresh Kumar, and Ben Kaldunski. 2022. *Development, Implementation, and Integration of a Holistic Solar Forecasting System for California*. California Energy Commission. Publication Number: CEC-500-2023-025.

TABLE OF CONTENTS

LIST OF FIGURES

Page

LIST OF TABLES

Page

EXECUTIVE SUMMARY

Introduction

Successfully integrating renewable resources, including wind and solar photovoltaics (PV), into electric power operations requires the ability to forecast the output of these resources in timeframes from less than an hour to days ahead. Fog and low-level clouds (stratus) affect solar brightness (irradiance) in California throughout the year, and shortcomings in predicting fog and stratus breakup constrain the accuracy and confidence of short-term solar irradiance forecasts. Methods to accurately forecast the timing of fog and marine layer burn-off will be required with more distributed and utility-scale solar energy resources in California.

As the world's 5th largest economy, California has ambitious energy goals. The California 100 percent Clean Energy Act, SB 100, set the goal of achieving 100 percent clean, carbon-free electricity by 2045. To meet this goal, the capacities of distributed and utility-scale PV systems will need to be significantly increased. However, due to the inherently variable and uncertain nature of solar power output, increased reliance on solar PV presents a challenge to grid operators, utilities, and other stakeholders. To accommodate solar energy in their operations, these stakeholders need tools and methods to help predict how solar output will vary over the next minutes, hours, and days. Accurate forecasts of solar output can maintain and improve grid reliability and economic efficiency. Predicting solar energy output, nevertheless, heavily relies on accurate solar irradiance forecasts. Fog and stratus affect solar irradiance in California throughout the year, and shortcomings in predicting fog and stratus dissipation currently constrain the accuracy and confidence of short-term (0 to 6 hour) solar irradiance forecasts. Thus, there is an urgent need to develop a California-specific version of Weather Research and Forecast Solar (WRF-Solar) model with improved physics and data assimilation for predicting fog and stratus dissipation.

Project Purpose

The primary goal of the project was to improve solar irradiance forecasting in time frames from less than one hour up to one day ahead, with a focus on those periods of most value to California grid operators and electric utilities. The project team achieved this goal through the use of: (1) existing boundary layer instrument networks and targeted deployment of new instruments in high solar penetration regions; (2) application of advanced machine learning prediction methods; (3) advancements in the type, amount, and method of data assimilated into numerical weather models; and (4) improvements in numerical weather model physics.

Another goal of the project was to address the holistic impact of solar irradiance variations on grid operations, including their direct effect on centralized and distributed solar-based power generation as well as their impact on regional and system-wide load through solar-induced variations in temperature and other parameters (e.g., environmental light availability). Improved solar irradiance predictions can provide value by improved solar energy output forecasts and improved prediction of temperature- or lighting-induced load variations. The impact and value of solar-based generation forecasting will significantly increase as solar generation capacity grows to much higher levels in response to the goals of California's Renewable Portfolio Standards.

The team developed an improved version of the WRF-Solar model and established a public dataset (with real-time data website) for the research community to facilitate further improvements to solar forecasting. The California WRF-Solar model developed in this project includes updated physics and data assimilation, new forecasting tools based on machine learning, and integration of new and existing data from a variety of meteorological instruments that were used during a 1.5-year field campaign. According to solar forecasting experts, the measurements and associated model improvements focused on key atmospheric phenomena that control the dissipation of valley fog and marine layer stratus are critical issues for utility-scale and distributed solar energy.

In addition to developing an improved WRF-Solar model for California, the team used data from the California Independent System Operator (California ISO) to evaluate the values of integrating the improved forecasts into the system operations. This work will lead to improvements in the WRF-Solar forecasting model for California and demonstrate the effectiveness of intelligent use of sensor technologies to aid electric grid operations as California moves forward with aggressive clean energy goals.

Project Approach

This project was carried out by a team comprised of members from the Electric Power Research Institute (EPRI), Sonoma Technologies, and UL Renewables/AWS Truepower. ASW Truepower's operational forecast models have been used by the California ISO and other stakeholders in the past; the improved forecasting model in this project was built based on the existing models used by AWS Truepower. Sonoma Technologies provided and installed one microwave radiometer for the project for a one-year period. EPRI has led various projects in terms of renewable forecast improvements and gird impacts analyses. Experiences acquired in these projects along with EPRI's computing capabilities were leveraged for simulations in the systems integration effort.

The project has four major technical components. The first component involved refining the targeted sensor network deployment and forecast specifications based on input from the technical advisory committee and project stakeholders. The project team selected and refined the locations for meteorological sensors by examining three factors: (1) the amount of PV generating capacity in the local area; (2) the frequency of significant stratus and fog events; and (3) regions of interest identified by California solar generation stakeholders, especially the investor-owned utilities (IOU) and California ISO. The objective was to identify areas of interest with a high frequency of stratus and fog events to inform sensor deployment. The second component involved developing a field data collection program. The San Joaquin Valley (primarily for winter fog), the San Francisco Bay Area (marine layer stratus), and the Los Angeles Basin (marine layer stratus) were identified as geographic regions of interest. The team designed a field data collection program to focus on improving data and forecasts for these areas, using existing instruments and project-specific deployments of new instruments to capture the key processes that influence fog and stratus dissipation. The ground-based instruments used in the field campaign included radar wind profilers with radio acoustic sounding systems, microwave radiometers (measures radiant energy), sodars (sonic detection and ranging–measures air turbulence), and ceilometers (measures cloud height). These remote sensing instruments use sound, light, microwave, and radio wave energy to measure the vertical structure of the atmosphere. They also provide key parameters including cloud

thickness, cloud base height, vertical wind shear, and inversion strength and height on a continuous basis for characterizing and predicting stratus dissipation.

The third component involved modeling improvement efforts to develop the California WRF-Solar model. WRF-Solar forecast improvements had three major phases: (1) targeting refinement of how the physical processes were represented in a Numerical Weather Prediction model; (2) applying advanced and customized methods for assimilating data into Numerical Weather Prediction models; and (3) applying machine learning methods to rapidly-update stratus and fog predictions.

The fourth component involved valuing improved solar forecasting, which assessed the value of improved solar forecasts and the integration of improved WRF-Solar forecasts into grid operations. The team assessed the economic and reliability values of improved solar forecasts through production cost modeling simulations.

The technical advisory committee was also put together to assist the project process. The members included experts from the California ISO, Clean Power Research, National Oceanic and Atmospheric Administration, Pacific Gas and Electric Company, and Southern California Edison. Four technical advisory committee meetings were held at various stages of the project to share results, methods, and preliminary results from each project task.

Project Results

The team completed a measurement program using ground-based atmospheric boundary layer sensors from December 2017 through March 2019 to support improvements in predicting fog and stratus dissipation in high solar penetration regions of California. The team collected unique data throughout California for several dozen marine stratus days and about one dozen radiation fog days. The measurement program involved augmenting existing sensor networks with new sensor deployments. The instrument network consisted of five radar wind profilers, seven sodars, six ceilometers, and two radiometers spread across ten measurement sites.

The key project results are focused on the following aspects:

1. *Locating Sodar and RASS Instrumentation and Collecting Data*: The team successfully integrated the existing sensor networks with new ones. This process required significant coordination between the project team and data providers to arrange site access and data sharing logistics, and this coordination allowed for unique data to be collected at a substantial cost savings compared to acquiring, siting, and operating new instruments. This successful measurement program can serve as a model for coordinating similar efforts in the future.
2. *Solar Forecasting Improvement*: The project team optimized key numerical weather prediction sub-models in weather research and forecasting to improve numerical simulation of the formation and dissipation of stratus and fog in both the marine layer and surface-based radiation fog scenarios in California. Specific components of the Weather Research and Forecasting-Solar physics sub-models that have the most impact on fog formation and dissipation were identified and optimized to improve forecast performance over a representative sample of cases. This process involved three steps: (1) conducting numerical weather prediction sensitivity experiments to evaluate errors and identify areas of improvement; (2) identifying the best Weather Research and

Forecasting-Solar configuration for fog and stratus forecasting in California to serve as the baseline weather research and forecasting-Solar configuration, and (3) refining the physics in the baseline Weather Research and Forecasting-Solar configuration. The results showed a slight overall improvement in forecast skill; however, the small change in the forecast outcome suggested that point measurements at a handful of locations are not likely to substantially improve forecasts above their already high skill beyond a few hours of forecast initialization.

3. *Using Machine Learning Models to Predict Cloudiness and Solar Irradiance*: The project team developed a preliminary cloud or clear sky machine learning prediction model for cloudiness. The Random Forest and XGBoost algorithms were used to evaluate the forecast performance relative to a persistence forecast model–a forecast that the current weather condition will persist and that future weather will be the same as the present. The machine learning models yielded reasonable results at predicting cloudiness and solar irradiance, with a forecast accuracy of greater than 95 percent. The XGBoost model performed slightly better than the Random Forest model.
4. *Quantifying the Value of Improved Solar Forecasting*: Two methods for quantifying the value of solar power forecasting were used: the historical data analysis method, and the production cost modeling simulation method. The former does not need detailed modeling of the electric power grid since it tries to build a relationship between the solar forecasting error and the market performance through historical operating data, whereas the latter requires detailed grid modeling. Results from the first method showed that there is not a simple correlation between the solar forecast error and the evaluation metrics. It is difficult to quantify the value of solar forecasting from studying and analyzing the historical data only. The Production Cost Modeling results show that with 20 percent solar forecast accuracy improvement in day-ahead, the fuel cost and startup cost of thermal units in the system can reduce by between 0.06 percent and 3 percent, depending on test systems. In addition, the violations on area balancing and reserves were reduced with improved solar forecast accuracy.

Technology Transfer and Advancing the Research to Market

This project relied on robust multi-disciplinary collaboration between technical experts in data science, meteorological measurement and forecasting, and electric grid operations to achieve core research objectives.

The project team delivered information through presentations (including at the 100th American Meteorological Society Annual Meeting in January 2020), interim project reports, and post-meeting reports that included question and answer responses. These meetings provided vital feedback to the research team that guided future activities. In addition to technical advisory committee meetings, a real-time data website was set up and maintained throughout the project to visualize data collected from all meteorological instruments during the field campaign. During the project timeframe, this website was available to research team members and project stakeholders (it was deactivated after the completion of the project). Input from California ISO and other stakeholders was also solicited throughout the project regarding solar forecast value assessment and integration into grid operations. This report along with final meeting materials and fact sheets will also be made publicly available by the CEC.

Benefits to California

The study provided the following benefits to California and its ratepayers:

A California-specific version of Weather Research and Forecasting-Solar forecasting model with improved physics and data assimilation was developed for predicting fog and stratus dissipation to improve the accuracy of solar generation predictions. This will be beneficial to meet California's ambitious energy goals, because fog and low-level clouds affect the amount of solar energy generated.

The benefits of improved fog and low-level cloud forecasting to the solar power systems are substantial with test results showing monthly fuel cost savings ranged from $123,486 to $902,929 when the solar generation forecast was improved by 20 percent, depending on which forecasting model was used. These savings translate into energy procurement cost savings for IOUs and lower electricity rates for end-use customers. As the number of solar installations continue to increase, the benefits of improved forecasting that lead to more efficient bulk power system operations will become more pronounced.

The project team also compared the grid impacts of solar forecasting improvement and energy storage resources. Simulation results from the modified California ISO test system show that the economic benefit of 20 percent solar forecasting improvement in day-ahead is close to that of adding a 25 MW battery storage resource to the system. However, 20 percent solar forecasting improvement in day-ahead brings significantly higher reliability benefit to the grid than adding 25 MW battery resources, where the reliability benefit was measured by the percentage of balancing violation reductions compared with the base case. The value of the metric (balancing violation reductions) was 54 percent for solar forecasting improvement and 2.5 percent for adding 25 MW batter storage. Note that 25 MW battery storage only accounts for a small portion of the total installed capacity, thus the reliability benefit was relatively small. (If more batteries were added, the benefits to the grid would be higher, but this is outside the scope of this research.) In addition, considering the investment cost and environmental impacts of building a battery storage resource, the solar forecasting improvement approach is (likely) less expensive and has almost no environmental concerns. This will bring additional benefits to California ratepayers.

CHAPTER 1: Introduction

Overview and Background

To meet California's ambitious energy goals, the capacities of distributed and utility-scale solar photovoltaic (PV) systems must be increased. Because of the inherently variable and uncertain nature of solar power output, however, increased reliance on solar PV presents a challenge to electricity grid operators, utilities, and other stakeholders. To accommodate solar energy in their operations, stakeholders need tools and methods to help predict how solar output will vary in the next minutes, hours, and days. Accurate forecasts of solar output can maintain and improve grid reliability and economic efficiency. Fog and stratus affect solar irradiance in California throughout the year, and shortcomings in predicting fog and stratus dissipation currently constrain the accuracy and confidence of short-term (0 to 6 hour) solar irradiance forecasts.

A wealth of meteorological data is currently used to initialize operational Numerical Weather Prediction (NWP) forecasts. However, the availability of boundary layer wind, temperature, and moisture profiles in the observation networks is limited. Targeted deployments of ground-based boundary layer sensors such as ceilometers, wind profilers, and microwave radiometers, have shown promise for improving local and regional NWP forecasts for wind energy applications (Bianco et al., 2019; Wilczak et al., 2019; Cooperman et al., 2018; Wilczak et al., 2015, 2019). For solar energy applications, the timing, spatial extent, depth, and dissipation of stratus and fog is difficult to predict (Kann et al., 2015; Gilles et al., 2010), but fog forecasting accuracy has been improved through improved model physics (Wilson and Fovell, 2018), data assimilation (Wang et al., 2014), and machine learning methods (Marzban et al., 2007; Bartokova et al., 2015). In addition, the Weather Research and Forecasting (WRF) model was customized for predicting solar irradiance as part of a recent solar forecasting improvement project supported by the Department of Energy. This customized version of WRF, known as WRF-Solar, includes an improved representation of the cloud-aerosol-radiation system (Jimenez et al., 2016) to facilitate more accurate predictions of solar irradiance.

The main goal of this research project was to develop a California-specific version of the WRF-Solar forecasting model with improved physics and data assimilation for predicting fog and stratus dissipation to improve the accuracy of solar generation predictions. The project implemented a measurement program involving targeted deployment of ground-based atmospheric boundary layer sensors in high solar penetration regions to augment existing meteorological monitoring networks and provide robust data to support data assimilation and model evaluation. The team used the data collected during the field campaign to support the application of machine learning algorithms to improve very short-term (0 to 2 hour) solar forecasting performance and assess the incremental skill added by including boundary layer sensor data. The impact and value of solar-based generation forecasting will significantly increase as solar generation capacity grows to meet the goals of California's aggressive Renewable Portfolio Standards (RPS). The research team collaborated with the California Independent System Operator (California ISO) and the investor-owned utilities (IOUs) to

identify the look-ahead periods and forecast parameters of greatest value to operational decision-making.

The project also sought to address the holistic impact of solar irradiance variations on grid operations, including its direct effect on centralized and distributed solar-based power generation. This goal served to ensure that improvements in solar forecasting were properly evaluated and integrated into decision-making processes, and that the value of improved forecast performance was estimated using robust and appropriate methods. Work completed under this project built on existing forecasting services that project team members currently provide to California ISO and provided an innovative solar power forecast solution for California stakeholders that synergizes with existing wind power forecasting techniques and includes a California-specific version of WRF-Solar.

Project goals and objectives

The primary goal of the project was to improve upon solar irradiance forecasting in time frames from less than one hour to one day ahead, with a focus on those periods of most value to system operations. We provided an improved version of the WRF-Solar model for California, and a public dataset for the research community to facilitate further improvements to solar forecasting. The overall goal was achieved through the following objectives: (1) deploy existing and new instrumentation to measure data related to solar irradiance, in particular fog and marine layer, in four regions across California; (2) develop forecasts of solar power and other weather-related variables that can inform system operations to deliver an improved version of WRF-Solar targeted on California to California ISO and the IOUs based on their specifications; (3) measure the improvement in forecast performance and verify the improvement in Root Mean Square Error for the relevant time horizons; and (4) create a methodology and deliver requisite datasets to measure the value of improved forecasts.

Technology Approach

The project team significantly improved the state-of-the-art for solar irradiance forecasting in California with a focus on stratus and fog dissipation scenarios by building on previous and ongoing work. This was achieved through the use of: (1) existing boundary layer instrument networks and targeted deployment of new instruments in high solar penetration regions; (2) application of advanced machine learning prediction methods; (3) advancements in the type, amount, and method of data assimilated into numerical weather models; and (4) improvements in numerical weather model physics. The instruments, including ceilometers, radiometers, sodars, radar wind profilers, traditional meteorological instruments, and satellite instruments, were used to characterize stratus, develop tools to predict stratus burn-off time, improve numerical models, and improve model initial conditions via real-time data assimilation.

The first part of the project focused on refining the field measurement network based on feedback from the technical advisory committee (TAC) and electric utilities, carrying out field data collection, and formulating specifications for the research team's forecast improvement efforts. The field data collection campaign launched in December 2017 and ran through March 2019 and provided robust meteorological data to: (1) characterize meteorological processes that influence fog and stratus cloud dissipation; and (2) improve short-term (0 to 6 hour) forecasts of fog and stratus cloud dissipation. To help meet these objectives, the project team

leveraged existing instrumentation networks and installed additional instruments to collect data at five core study sites and several supplemental (non-core) study sites across California. The sites were located in the Central Valley, the San Francisco Bay Area, and the Los Angeles Basin, which are areas of high solar penetration that experience frequent stratus cloud or fog events.

The formation, evolution, and dissipation of fog and stratus is driven by complex interactions between large-scale atmospheric forcing (advection and subsidence), mesoscale forcing (for example land/sea breezes and mountain/valley flows), boundary layer processes (surface fluxes and turbulence), and cloud radiative and microphysical processes (such as liquid water content, cloud albedo, cloud top radiative cooling) (Koracin et al., 2014; Gultepe, 2007). Fog and stratus are often capped by a temperature inversion, which can be surface-based or elevated, and can vary in height and strength. Solar radiation drives cloud dissipation by heating the ground surface and inducing boundary layer mixing that erodes the cloud from below. Cloud dissipation is modulated by large-scale flows, surface vegetation, soil moisture, and local terrain.

Generally, fog and stratus dissipation are controlled by a few key parameters that can be readily measured or derived from boundary layer instruments: (1) solar radiation; (2) inversion height and strength; (3) cloud base height; (4) cloud thickness and liquid water content; and (5) boundary layer winds, temperature, and moisture. The field measurement program collected data to capture the key processes that influence stratus dissipation.

Figure 1: Key Parameters that Affect Cloud Dissipation

Source: Sonoma Technology, Inc., 2022

Figure 1 shows the key parameters that affect cloud dissipation and the instruments that were used to measure these parameters in the field program. These instruments included radar wind profilers (RWP) with radio acoustic sounding systems (RASS), microwave radiometers, sodars, and ceilometers, as well as traditional surface meteorological instruments. The red line in the diagram shows an idealized vertical temperature profile in a marine boundary layer capped by a subsidence inversion. The blue arrows are an idealized representation of the vertical wind profile and wind shear. Other important processes not shown include cloud-top radiative cooling, surface heating and convective turbulence, terrain effects, and advective forcing. Instruments used to observe these processes are noted in parentheses.

The second part of the project focused on physics-based model refinements, data assimilation, and the application of machine learning algorithms to improve solar forecasting performance by using data collected during the field campaign. Work on physics-based model refinement optimized key NWP sub-models for the numerical simulation of the formation, maintenance, and dissipation of stratus and fog in marine layer and surface-based radiation fog scenarios in California. Sensitivity analysis was performed for intra-day (0-24 hours) WRF-Solar stratus and fog forecasts for a range of key physical parameters embedded in a physical sub-model for California based on several dozen marine layer stratus days and approximately one dozen radiation fog days.

Data assimilation research activities focused on customizing the WRF data assimilation configuration to develop a WRF-Solar model initialization that was optimal for California stratus and fog forecasting. The best NWP model initialization and customized data assimilation configuration for California fog and stratus forecasting was identified by analyzing a set of initialization datasets available from the National Oceanographic and Atmospheric Administration's (NOAA) NWP models. Analysis included a comparison of key attributes (for example, cloud depth, cloud top, horizontal cloud extent, inversion height, soil moisture, soil temperature, sea surface temperature) in the initial model state to those obtained from the project sensors and other measurement devices. A comparison of WRF-Solar forecast results using the different model initialization datasets and data assimilation configurations was also completed. Systematic issues with the initialization data from the baseline source were identified to formulate a data assimilation approach and customized WRF-Solar initialization procedure software.

Machine learning approaches were applied to time series data obtained from project sensors and other measurement sources to address very short-term (15 minute to 2-hour forecast horizons) predictions of stratus cloud and solar irradiance. The objective was to formulate an approach that uses the latest data to provide useful forecast updates more quickly than is possible with current NWP technology. Meteorological data collected from project sensors were used as independent variables to predict cloud cover conditions (clear sky, stratus, transition from stratus to clear sky, and transition from clear sky to stratus) and solar irradiance, with a focus on predicting the onset of cloud dissipation. Data withheld from the training dataset were used to evaluate performance for a range of time lags up to 120 minutes into the future. In addition, sensitivity analysis was performed to assess the predictive power provided by each input dataset.

The third part of the project focused on developing a method and dataset to evaluate baseline solar forecast performance for comparison against the value of forecast improvement based on aspects such as time of day and ramping conditions. Research activities also focused on quantifying improvements in forecast accuracy to determine the benefits of those improvements to various stakeholders, particularly electric utility ratepayers. Those benefits included reduced system operating cost, reduced reserve violations, and reduced renewables curtailment, which will finally turn into dollar values for the ratepayers.

CHAPTER 2:
Project Approach

The studies in this project mainly contain the following technical topics: (1) field data collection program; (2) physical and statistical prediction modeling; (3) machine learning for very short-term predictions; (4) solar forecast performance analysis; (5) solar forecast value assessment; and (6) grid impacts assessment of improved solar forecasting versus energy storage resources. The overviews of the approaches used in each topic are summarized in what follows, while the details of the approaches are shown in the appendices.

Field Data Collection

The research team developed a field measurement program that augmented existing meteorological monitoring networks and provided robust data to support improvements to models used for forecasting fog and stratus conditions in California. The measurement program involved targeted deployment of ground-based atmospheric boundary layer sensors in high solar penetration regions of California. The field program began in December 2017 and concluded in March 2019. The meteorological data obtained were integrated into NWP models and statistical techniques to improve short-term (0 to 6 hour) forecasts of fog and cloud stratus formation and dissipation. Ultimately, these data supported the development of an improved version of the WRF-Solar model, focused on California (Zack and Craig 2017).

Figure 2: Study Sites Used in the Field Measurement Program

Red sites are the five core sites for this project (LAX, Irvine, Visalia, Fremont, and Benicia). Blue sites are the supplemental (non-core) sites.

Source: Sonoma Technology, Inc., 2022

Table 1 summarizes the study sites. The five core sites had some combination of a sodar, an RWP/RASS, a ceilometer, a radiometer, and a surface meteorological station. In most cases, these sites had existing instruments that were leveraged during the project. The core sites were the primary focus of the field program. In addition to the five core sites, several supplemental sites also had instruments that were beneficial to this project and were therefore included in the field program. The organizations that own the data, sites, and/or instruments are the South Coast Air Quality Management District (SCAQMD), the San Joaquin Air Pollution Control District (SJVAPCD), the Sacramento Metropolitan Air Quality Management District (SMAQMD), NEXTracker, Inc. (NEXTracker), and Sonoma Technology, Inc. (STI). Each site owner granted permission to use data and/or access the monitoring site to deploy and maintain equipment.

Table 1: Study Sites Used in the Field Measurement Program

Field Site	Site Owner	Core/Supplemental Site	Operating Season
Los Angeles (LAX)	SCAQMD	Core	All Year
Irvine	SCAQMD	Core	Warm Season
Visalia	SJVAPCD	Core	Cool Season
Fremont	NEXTracker	Core	Warm Season
Benicia	STI	Core	All Year
Ontario	SCAQMD	Supplemental	All Year
Moreno Valley	SCAQMD	Supplemental	All Year
Pacoima/Whiteman Airport	SCAQMD	Supplemental	All Year
Sacramento/Bruceville	SMAQMD	Supplemental	Cool Season
Richmond	STI	Supplemental	All Year

SCAQMD – South Coast Air Quality Management District; SJVAPCD – San Joaquin Valley Air Pollution Control District; SMAQMD – Sacramento Metropolitan Air Quality Management District; STI – Sonoma Technology, Inc.

Source: Sonoma Technology, Inc., 2022.

To maximize project resources, not all sites and instruments operated during the entire field program. Instruments deployed in Irvine and Fremont operated only during the warm season (April through October) when coastal stratus is more prevalent, while instruments used in Visalia and Sacramento operated only during the cool season (November through March) when inland radiation fog is most prevalent. Instruments at the other sites operated throughout the year.

Instrument Details and Data Examples

The ground-based remote sensing instruments used in the field measurement program included radar wind profilers (RWP) with radio acoustic sounding systems (RASS), microwave radiometers, sodars, and ceilometers. These instruments provided key parameters on a continuous basis for characterizing and predicting stratus dissipation including cloud thickness, cloud base height, vertical wind shear, and inversion strength and height. Other parameters such as ground level solar radiation, surface energy flux, and horizontal advection were obtained using traditional surface measurements. Cloud brightness and spatial distribution were obtained from existing Geostationary Operational Environmental Satellite (GOES) products. The next generation of GOES, GOES-R, did not become operational during the field program, therefore, the research team was not able to incorporate GOES-R data products into the project.

The field sites had various combinations of instruments that measured surface and upper-air meteorological parameters. Table 2 lists details about the existing and deployed instruments at the five core sites.

Table 2: Instruments at Core Project Sites

Instrument	Measurement	Los Angeles	Irvine (Warm Season)	Visalia (Cool Season)	Fremont (Warm Season)	Benicia
RWP	Wind profiles	Vaisala LAP 3000 (existing)	Vaisala LAP 3000 (existing)	Vaisala LAP 3000 (existing)	—	—
RASS	Temperature profiles, inversions	Vaisala LAP 3000 (existing)	Vaisala LAP 3000 (existing)	Vaisala LAP 3000 (existing)	—	—
Sodar	Wind profiles	ASC s4000 (existing)	ASC s4000 (existing)	—	ASC s2000 (added)	ASC s2000 (existing)
Ceilometer	Boundary layer height, cloud base height	Vaisala CL31 (existing)	Vaisala CL51 (added)	Vaisala CL31 (added)	Vaisala CL31 (added)	Vaisala CL31 (existing)
Radiometer	Liquid water/cloud thickness, temperature and relative humidity profiles	Radio-metrics MP-3000A (existing)	—	Radio-metrics MP-3000A (added)	Radio-metrics MP-3000A (added)	—
Surface Meteorology	Winds, temperature, relative humidity, solar radiation	Existing	Existing	Added	Added	Added

Source: Sonoma Technology, Inc., 2022

The project team used new sensors at Visalia, Irvine, Fremont, and Bruceville/Sacramento during the field program. Visalia was intended as a cool season site to collect observations of Central Valley radiation fog. A microwave radiometer, ceilometer, and surface meteorological instrumentation were added at Visalia to augment the existing RWP/RASS and sodar instruments. Fremont was intended as a warm season site to collect observations of marine stratus in the San Francisco Bay Area. The Fremont site did not have existing instrumentation and it was the one entirely new field site for this project. A radiometer, sodar, ceilometer, and surface meteorological instrumentation were added at the Fremont site. Irvine was also intended as a warm season site, and a ceilometer was added there to augment the existing RWP/RASS, sodar, and surface meteorological instruments. No new instrument deployments were originally planned for the Bruceville/Sacramento supplemental site, but a microwave radiometer was added alongside the existing ceilometer in December 2018 to take advantage of an opportunity to collect additional observations of radiation fog in the Central Valley. Table 3 shows instruments at the supplemental sites.

Table 3: Instruments at Supplemental Project Sites

Instrument	Measurement	Ontario	Sacramento/ Bruceville (cool season)	Moreno Valley	Whiteman/ Airport Pacoima	Richmond
RWP	Wind profiles	Vaisala LAP 3000 (existing)	Vaisala LAP 3000 (existing, but not operable)	Vaisala LAP 3000 (existing)	—	—
RASS	Temperature profiles, inversions	Vaisala LAP 3000 (existing)	Vaisala LAP 3000 (existing but not operable)	Vaisala LAP 3000 (existing)	—	—
Sodar	Wind profiles	ASC s4000 (existing)	—	—	ASC s4000 (existing)	ASC s2000 (existing)
Ceilometer	Boundary layer height, cloud base height	—	Vaisala CL31 (added)	—	—	—
Radiometer	Liquid water/cloud thickness, temperature and relative humidity profiles	—	Radiometrics MP-3000A (added)	—	—	—
Surface Meteorology	Winds, temperature, relative humidity, solar radiation	Existing	—	Existing	Existing	—

Source: Sonoma Technology, Inc., 2022

Table 4 summarizes key information about the instruments used in the field program. The science behind these instruments and data examples are described in the following sections.

Table 4: Measurements Collected During the Field Study

Instrument / Manufacturer	Parameter(s)	Measurement Height(s) above ground level (m)	Vertical Resolution (m)	Frequency (min)
Mini-Sodar (ASC Sodar 4000)	Wind speed and direction	~20 to 200	~40	15
Sodar (ASC Sodar 2000)	Wind speed and direction	~80 to 600	~30	15
Microwave Radiometer (Radiometrics MP-3000A)	Temperature, humidity, and liquid water	~10 to 10,000	~50 below 500; 100 between 500 and ~2000; 250 above 2000	6
RWP (Vaisala LAP 3000)	Wind speed and direction	~120 to 3500	~100	55
RASS (Vaisala LAP 3000)	Virtual temperature	~120 to 1500	~60	5 at top of hour
Ceilometer (Vaisala CL31 or CL51)	Height of a cloud base, mixing height	~0 to ~7,600	5	1
Surface Meteorology (various manufacturers)	Temperature, wind speed & direction, relative humidity, surface solar radiation	2 to 10	--	1-60

Source: Sonoma Technology, Inc., 2022

Details of ASC Sodar 4000 (Mini-SODAR)

The mini-sodar consists of a phased array of emitters (speakers) that steers acoustic pulses so that the individual components of the wind (two horizontal and one vertical, or u, v, and w) can be resolved. After each pulse, a receiver measures the small amounts of the transmitted sound that are scattered back toward the sodar (referred to as "backscattering"). These backscattered signals are received at a slightly different frequency than the transmitted signal. This difference is called the Doppler frequency shift and is directly related to the velocity of the air moving toward or away from the sodar along the direction the beam is pointing. The radial velocity measured by the tilted beams is the vector sum of the horizontal motion of the air toward or away from the sodar plus any vertical motion present in the beam. Using trigonometry, the three-dimensional meteorological velocity components (u, v, w), wind speed, and wind direction are calculated from the radial velocities.

The mini-sodar operates at a frequency of approximately 4500 Hz and the emitted sound is ~95 dbA. Because it emits noise, a mini-sodar must be located away from nearby residences. Furthermore, a mini-sodar should be located in an area with very infrequent ambient noise near the 4500 Hz frequency because the mini-sodar "listens" to reflections of its sounds off of the atmosphere. The mini-sodar can be powered using batteries and solar power or AC power if available. A mini-sodar located at a field site is shown in Figure 3.

Figure 3: Mini-sodar located at a field site

Source: Sonoma Technology, Inc., 2022

Details of ASC Sodar 2000

The Sodar 2000 uses three parabolic dishes with a compression driver at the focal point of each dish to generate audible acoustic pulses (e.g., chirps or beeps every 4 to 6 seconds). The parabolic dishes are situated so that two orthogonal horizontal wind components (u, v) and

one vertical wind component (w) are sampled to compute the reported wind profile. Just as with the mini-sodar, a receiver measures the small amounts of the transmitted sound that are scattered back toward the sodar. These backscattered signals are received at a slightly different frequency than the transmitted signal. This difference is called the Doppler frequency shift and is directly related to the velocity of the air moving toward or away from the sodar along the direction the beam is pointing. The radial velocity measured by the tilted beams is the vector sum of the horizontal motion of the air toward or away from the sodar plus any vertical motion present in the beam. Using trigonometry, the three-dimensional meteorological velocity components (u, v, w), wind speed, and wind direction are calculated from the radial velocities.

The Sodar 2000 operates at a frequency of approximately 1800 Hz and the emitted sound is ~90 dbA. Because they emit sound, sodars will be located as far away from nearby residences as possible. A Sodar 2000 located in the field is shown in Figure 4.

Figure 4: Sodar 2000

Source: Sonoma Technology, Inc., 2022

Details of the Radiometrics Microwave Profiler (Radiometer)

The Radiometrics MP-3000 microwave profiler is a hyperspectral microwave receiver (radiometer). This instrument observes microwave energy emitted by the atmosphere, which is converted to brightness temperatures using Planck's Law. Algorithms convert radiometer observations to temperature, humidity, and liquid water profiles. The vertical profiles are measured from about 50 to 10,000 m above ground level (agl). The vertical resolution of the data varies with height: the resolution is 50 m below 500 m agl, 100 m between 500 and 2000 m agl, and 250 m above 2000 m agl. Because the radiometer scans the atmosphere, it should be located at a site with clear views of the sky to about 10 degrees above the horizon. Due to significant power consumption, AC power must be used to operate the instrument. A radiometer is shown in Figure 5.

Figure 5: Radiometrics radiometer

Source: Sonoma Technology, Inc., 2022

Details of the Vaisala Ceilometer

The Vaisala CL31 ceilometer works by vertically emitting an eye-safe laser beam and detecting the reflection of the beam by particles with a receiver. The continuous reflectivity (or backscatter) data are available from about 0 to 7,600 m agl; for boundary layer characterization, the sensitivity is adequate up to approximately 3,000 m agl. Sub-hourly boundary-layer heights with a vertical resolution of 5 m are derived from the backscatter data. Figure 6 shows a ceilometer.

6: Vaisala CL31 ceilometer located on Chevron's ST-52B oil platform in the Gulf of

Mexico

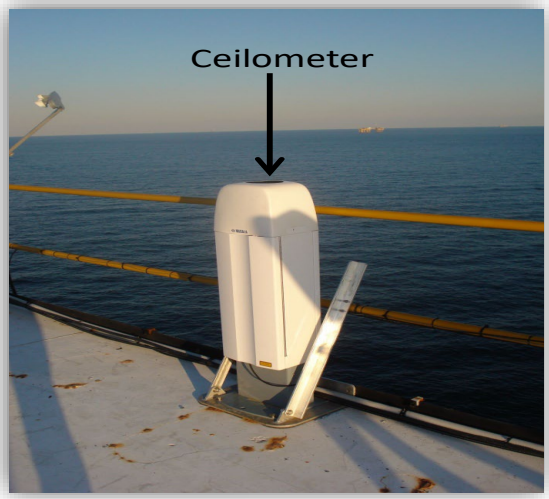

Source: Sonoma Technology, Inc., 2022

Physical and Statistical Prediction Modeling

This section describes research activities performed to improve forecast accuracy of the Weather Research Forecast (WRF) model. WRF is an open-source community NWP model that was jointly developed by the National Center for Atmospheric Research (NCAR) and NOAA with major ongoing contributions from the global atmospheric science community. The objectives of this task were to: (1) customize the representation of physical processes in a NWP model for California stratus and fog forecasting; (2) customize advanced NWP data assimilation methods for California stratus and fog forecasting; (3) apply machine learning methods for rapid update of stratus and fog prediction based on the most recent sensor data; and (4) construct a method to optimally combine the physics-based and statistical forecasts and evaluate the composite forecasts over a one-year period. Research activities carried out to achieve these objectives are described in the following sections.

Solar Forecast Specifications

T four sets of forecast specifications targeted for development, refinement, and evaluation were: were (1) definition of the forecast target variables; (2) the time specifications of the forecasts; (3) the locations and areas that will be forecasted; and (4) the targeted end users of the forecasts.

Two types of forecasts were considered in this project: site-based and area-based. Site-based forecasts were developed and evaluated for specific target locations where sensors measured each of the target forecast variables. Area-based forecasts were developed on a high-resolution grid over the target areas of interest. Sensor data was not available at every grid point and the values of the forecast variables were therefore inferred from satellite-based data or nearby ground-based measurements.

Site-based forecasts were developed for the project sensor deployment sites. The presence of sensors at each data collection site provided an opportunity to produce and evaluate predictions for a more comprehensive set of variables than is possible for locations without ground-based sensor data. This facilitated a deeper understanding of the impact of each piece

of data on forecast performance and how to optimize the forecast system configuration at locations without a comprehensive sensor dataset. The full list of target variables for the site-based forecasts are listed in Table 5.

Table 5: Variables for Site-Based Forecasts

Variable	Units
Global horizontal solar irradiance	Watts/m^2
Existence of fog and/or stratus	Yes/No
Stratus/Fog dissipation time	HH:MM PST
Ceiling height	m AGL
Liquid water path length	Kg/m^2
Temperature inversion height	m AGL
Inversion strength	°C/m
Boundary layer temperature profile	°C at 50-100 m intervals from surface to 1000 m
Boundary layer relative humidity profile	% at 50-100 m intervals from surface to 1000 m
Boundary layer wind speed and direction profile	m/s and ° from N at 50-100 m intervals from surface to 1000 m
Wind shear across temperature inversion	s^{-1}

Source: UL Renewables/AWS Truepower, 2022.

Two targeted look-ahead time scales were considered for the site-based and area-based forecasts. The first-time scale was an intra-day period that extended from the forecast issue time through sunset. The time specifications for the intra-day forecasts included: forecast issue times of 1 am to 12 pm local time; forecast look ahead periods ranging from the forecast issue time to sunset; and the forecasts were updated every 30 minutes at a time resolution of 15 minutes. These forecasts were meant to provide frequent updates about the extent and expected dissipation time of fog and stratus for the current day. The predictions were heavily based on data from ground- and satellite-based sensors. Modest weight was given to the output from rapid update NWP models, mostly for the longer look-ahead times within this time scale.

The second look-ahead time scale was for day-ahead forecasts. The look-ahead period covered the period from 1 am local time to sunset of the calendar day after the day the forecast was issued. The full set of forecast specifications included: forecast issue times of 5 am-11 am-5 pm local time; forecast look-ahead periods ranging from 1 am to sunset of the following day; and the forecasts were updated every six hours with time resolution granularity of 15 minutes. These forecasts were meant to provide a day-ahead outlook for the expected areal coverage of fog and stratus as well as its anticipated dissipation times. The forecasts were heavily based on the output from regional and global NWP models. However, the outputs were statistically adjusted using machine learning algorithms using data from ground- and satellite-based sensors to reduce the systematic errors in the NWP forecasts. Grid-based forecasts at 1 kilometer (km) resolution of the area-based target variables were produced for three target regions and location-specific forecasts of the site-based variables were produced for the core and supplemental measurement sites in each target region.

Physics Based Model Refinement

Research activities in this technical area optimized key NWP sub-models in WRF to improve numerical simulation of the formation and dissipation of stratus and fog in the marine layer and surface-based radiation fog scenarios in California. WRF was customized for predicting the three major components (global, direct, and diffuse) of solar irradiance as part of a solar forecasting improvement project supported by the U.S. Department of Energy. This customized version of WRF is known as "WRF-Solar" and it includes modifications to the short-wave radiation, aerosol, and water microphysics sub-models to facilitate more accurate predictions of solar irradiance. WRF-Solar served as the starting point for NWP refinements undertaken as part of this research project.

Specific components of the WRF-Solar physics sub-models that have the most impact on fog formation and dissipation were identified and optimized to improve forecast performance over a representative sample of cases.

To test the dependence of model results on the strength of cloud-top entrainment, experiments were performed in which the code of the Yonsei University (YSU) scheme was changed and the WRF model recompiled to use the new code. These experiments are summarized in Table 6. The experiments were performed over several days in September 2018. The project performed runs using two alternative values of the parameter a2, designed to give stronger cloud-top mixing (and thus more rapid break-up of boundary layer clouds) and a set of runs with a2 set effectively to zero and the entrainment flux effectively set equal to 0.25 times the first term in the equation, to explore the impact of weaker cloud-top mixing, and thus more persistent boundary layer clouds. Details of the physics-based model refinement steps and results are shown in Appendix B.

Table 6: Experiment Names and Descriptions

Experiment	Description
Baseline	RRTM Radiation & YSU Boundary Layer with Top-Down Mixing
YSU Top-Down Mixing Off	RRTM Radiation,YSU *without* Top-Down Mixing
YSU a_2=15	As in Baseline, but with YSU scheme modified for stronger top-down mixing
YSU a_2=30	As in Baseline, but with YSU scheme modified for very strong top-down mixing
YSU reduced w_e	RRTM Radiation,YSU with Top-Down Mixing

Source: UL Renewables/AWS Truepower, 2022.

Machine Learning for Very Short-Term Predictions

This section describes the development and application of very short-term (15 minute to 2-hour forecast horizons) stratus cloud and solar irradiance prediction methods based on the application of machine learning (ML) algorithms (McGovern, 2017, 2019) to time series data obtained from project sensors and other measurement sources. This work formulated an approach that uses the latest data to provide useful forecast updates more quickly than is possible with current NWP technology. Meteorological data collected from project sensors were used as independent variables to predict cloud cover conditions (clear sky, stratus, transition from stratus to clear sky, and transition from clear sky to stratus) and solar irradiance, with a focus on predicting the onset of cloud dissipation. Data withheld from the training dataset

were used to evaluate performance for a range of time lags up to 120 minutes into the future. In addition, sensitivity analysis was performed to assess the predictive power provided by each input dataset.

This work sought to address several research questions related to improving statistics-based solar radiation forecasting:

- Can boundary layer observations coupled with ML approaches improve very short-term forecasts of cloud and solar irradiance?
- Which of the selected ML approaches performs better?
- How much improvement in forecast skill (sensitivity, specificity, precision, and f1-score) can be achieved when including boundary layer measurements such as temperature, water vapor mixing ratio, and cloud liquid water content as predictors?
- Which sensors and parameters provide the most value in improving cloud and solar irradiance forecasts?
- How good are the predictions for a given range of time lags (15 minutes to 2 hours)?

Machine Learning Methods

The project team reviewed several ML methods to determine which algorithms may be well suited for predicting fog and stratus cloud dissipation. This review was based primarily on the research team's prior experience applying ML algorithms to meteorological forecasting problems, while also considering the specific forecasting problem being addressed and the type and amount of sensor data available for training. The project team selected the Random Forest (RF) approach and the extreme Gradient Boosting (XGBoost) ML approaches. Both approaches are known as "supervised" learning methods because they require a training dataset of known prediction outcomes to be effective at predicting future outcomes. Using artificial neural networks was considered, but the amount of sensor data from the field measurement program was insufficient to meet the large data requirement needs of neural network approaches.

The RF algorithm (Breiman, 2001) is an ensemble decision tree-based method that uses a bootstrap aggregating (bagging) technique to train the model. The bagging technique randomly samples the training dataset with replacement and fits trees to these samples. The fitted trees are then used to make predictions by averaging the predictions from all of the trees. Bagging reduces variance in predictions without increasing the bias in model fitting. Compared to a traditional decision tree algorithm, RF selects a random subset of the independent variables for splitting instead of considering all independent variables. This is to prevent the correlation between the trees if one or more independent variables are strong predictors for the dependent variable and thus are used in multiple trees. The scikit-learn python module (https://scikit-learn.org/stable/) was used to implement the RF algorithm on the project sensor data. The Random Forest Classifier function was used to predict cloudiness while the Random Forest Regressor function was used to predict solar irradiance.

The XGBoost algorithm (Chen and Guestrin, 2016) is a gradient boosted regression model that is optimized to be highly efficient, flexible, and portable. Gradient boosting builds a set of weak predictive models (also called weak "learners") one at a time. The first model, which might be a tree-based model or a simple linear regression model, predicts only the gross features of the data. Each successive model predicts successively subtler features of the data. In this manner, XGBoost iteratively combines weak predictive models into a stronger model as

the algorithm "learns" the error from the previous iteration. An important part of the gradient boosting algorithm is the regularization by shrinkage. The shrinkage technique multiplies each weak learner by a learning rate to prevent overfitting. In general, using a small learning rate improves the model performance. The scikit-learn python module was used to implement the XGBoost algorithm on the project sensor data.

Data Description

The project team developed, trained, and evaluated the ML-based forecasting approaches using meteorological data collected at the Fremont core site from August to November of 2018, and at the Los Angeles International Airport (LAX) core site from July 2017 to September 2018. Data from LAX that were available prior to the field measurement program for this project provided additional data for training and analysis. The analysis periods included 42 coastal stratus cloud events at Fremont and 105 stratus cloud events at LAX that were associated with a wide range of cloud base heights, cloud depths, spatial coverage, and cloud burn-off times. ML-based predictions of inland radiation fog in the San Joaquin Valley could not be developed because only 12 radiation fog cases occurred during the field measurement program, and this number was insufficient to develop robust ML-based predictions.

The instruments available at Fremont and LAX were previously summarized with both sites having a microwave radiometer that measured temperature, humidity, and cloud water profiles at 58 vertical layers from 0 to 10 kilometers (km) above ground level (agl). Both sites also had a radar wind profiler that measured vertical wind profiles (wind speed and direction) from 0 to 4 km agl. The LAX site also had a sodar that measured winds up to 600 meters (m) agl. Both sites had a ceilometer for measuring cloud base heights and boundary layer heights. Surface meteorological data and downward solar radiation data at 5-minute resolution from the Fremont site was used in the ML analysis. For LAX, surface temperature, wind, and humidity data at 2-minute time resolution from the nearby Automated Surface Observing System (ASOS) station were used. Solar radiation data at LAX were only available at hourly time resolution, so higher-resolution solar radiation data were interpolated from the hourly data.

In addition to the special sensor data at Fremont and LAX, the project team used surface meteorological data throughout California from the National Center for Environmental Information (NCEI) Integrated Surface Hourly database. Hourly pressure gradients were calculated between LAX and Daggett, between LAX and Ontario, between San Francisco International Airport (SFO) and Ukiah, and between SFO and Sacramento; these pressure gradients characterized large-scale meteorological conditions that could exert influence over the presence and persistence of marine stratus at Fremont and LAX.

Several processing steps were needed for quality control and to homogenize the input data in preparation for ML model development. Time series for each parameter were checked for skewness and to identify outlier and missing values. Because ML methods require complete data, missing data were imputed using temporal interpolation. When temporal interpolation was not feasible, the average value for the entire dataset was used. To prevent overfitting and to evaluate forecast performance, 70 percent of the data were randomly selected as the training dataset, and 30 percent of the data were withheld for testing and evaluation. For Fremont, there were 7,358 data records (a data record is all parameters at a given time). For

LAX, there were 32,453 records. All the performance metrics shown in Appendix B were calculated using the test dataset.

Cloud Data Classification

Two types of parameters were targeted for the ML-based models: stratus clouds and downward solar radiation at the ground. The solar radiation data can be used directly in the ML algorithms, but an objective approach is needed to identify and classify stratus clouds. Cloud base data from the ceilometer were used to identify the presence of stratus clouds. A 15-minute period was considered to be cloudy if the ceilometer reported a cloud base height below 2,000 feet agl for more than 50 percent of ceilometer data points (every 16 seconds) within the 15-minute period. Climatologically, cloud bases above 2,000 meters agl at Fremont and LAX are frequently not associated with marine stratus clouds, but the classification approach used here could miss some stratus cloud events associated with very deep marine boundary layers.

The transition from stratus conditions to clear skies is potentially more difficult to predict than binary cloud/no-cloud predictions but is highly relevant to forecasting solar electrical generation. Therefore, the binary cloud classification was expanded to a 4-class scheme (Table 7) to reflect the occurrence of stratus clouds (stratus or clear) at a particular time, and the transition between cloudy and non-cloudy states (stratus forming and stratus clearing) between two different times. These classifications (coded as 0-3) were used as the prediction goal for the ML models.

ML Application

The project team developed ML-based models to predict whether there would be stratus clouds at Fremont and LAX at a given time, and to predict how much solar radiation would be reaching the ground at Fremont. The project team conducted a preliminary analysis using both the RF and XGBoost algorithms for Fremont to predict cloudiness and solar radiation, with different time lags applied to evaluate forecast skill at different forecast horizons ranging from 15 minutes to 2 hours. The preliminary analysis used only the binary cloud classification (Classes 0 [Clear] and 3 [Stratus]) and excluded data from the Fremont radar wind profiler. The preliminary analysis confirmed the viability of the ML algorithms for predicting stratus clouds and solar irradiance, provided insights on the variables that may be important for predicting stratus clouds and solar irradiance, and defined refinements for subsequent algorithm development and analysis. Based on the results from the preliminary analysis, the project team conducted a more refined analysis with XGBoost for Fremont and LAX using all four classifications.

Table 7: Stratus Cloud Classification for the ML Analysis

Classification	Description	State at Current Time	State at Current Time Plus a Time Lag
0	Clear sky	Clear	Clear
1	Clear sky to stratus	Clear	Stratus
2	Stratus to clear sky	Stratus	Clear
3	Stratus	Stratus	Stratus

For each 15-minute period, the cloud state was determined for a current time and for a future time. Time lags ranging from 15 to 120 minutes into the future were investigated.

Source: Sonoma Technology, Inc., 2022.

Learning in ML algorithms is controlled by hyperparameters that are set prior to the start of the learning process. Table 8 describes the hyperparameters for the XGBoost algorithm**.** The process of selecting these optimal values is known as hyperparameter tuning. The preliminary analyses used default hyperparameter values. For the RF algorithm, the minimum sample for split selection was set at 2 and the number of estimators (number of trees) was set at 10. For XGBoost, the maximum depth of the trees was set at 6, the learning rate was set at 0.3, and the number of iterations was set at 100. The objective function used for predicting the binary classification was reg:regression.

Table 8: Hyperparameters Tuned for XGBoost

Hyperparameter	Distribution Used (Fremont)	Distribution Used (LAX)	Description
n_estimators	st.randint(3, 300)	st.randint(100, 1000)	Number of trees that can be built.
max_depth	st.randint(3, 40)	st.randint(3, 60)	The maximum depth of a tree.
learning_rate	st.uniform(0.05, 0.4)	st.uniform(0.01, 0.4)	Step size shrinkage used to prevent overfitting.
colsample_bytree	stats.beta(10, 1)	stats.beta(10, 1)	Percentage of features used by each tree.
subsample	stats.beta(10, 1)	stats.beta(10, 1)	Percentage of samples used per tree.
gamma	stats.uniform(0, 5)	stats.uniform(0, 5)	Regularization parameter for the algorithm.
reg_alpha	stats.expon(0, 50)	stats.expon(0, 50)	Regularization parameter for the algorithm.
min_child_weight	stats.expon(0, 50)	stats.expon(0, 50)	Minimum sum of instance weight needed in a child.

Source: Sonoma Technology, Inc., 2022.

The project team implemented hyperparameter tuning for the refined analysis. The optimal value of these hyperparameters cannot be known in advance and must be selected for each learning problem based on empirical observation of learning performance. For the refined analysis, the project team used the randomized Search CV algorithm implemented in SciKit Learn to tune hyperparameters for each modeling scenario. The tuning distributions used for each hyperparameter at Fremont and LAX are shown. A randomized grid search is preferred over a "brute-force" search over all possible hyperparameter values for computational efficiency. Given the multiple classifications (i.e., more than two classes), the objective function multi:softprob was used in XGBoost. The randomized Search CV function further used the negative log loss for scoring for hyperparameter selection.

For the refined analysis, the data counts across the four cloud classifications were unbalanced, as cloud transitions are much less frequent in the data compared to the "stratus" or "clear sky" data classifications. The unbalanced classifications can result in poor prediction performance for rare classifications. To address this issue, the team applied sample weights within XGBoost and calculated the weights for each record using the "balanced" method implemented in the SciKit Learn compute class weight function:

$$Sample\ weight\ for\ class\ i = \frac{Total\ sample\ number\ (all\ classes)}{Number\ of\ samples\ (class\ i) * Number\ of\ classes}$$

To assess the contribution of specific combinations of project sensor data to the ML-based predictions, the project team conducted a sensitivity analysis by withholding observations from each sensor and using the constrained dataset to train a new model. The sensitivity scenarios are described in Table 9. The baseline scenario only uses synoptic meteorological data, and no project sensor data. All other scenarios include data from one or more project sensors. Withholding occurred after feature selection, and hyperparameter tuning was performed for each sensitivity step.

Table 9: Description of Sensitivity Scenarios for the Refined ML Analyses

Scenario	Synoptic (Baseline) Meteorolog-ical Data	Surface Meteorology	Ceilo-meter	Radio meter	Wind Profil-er	No. of Features (Fremont)	No. of Features (LAX)
baseline	✓					4	4
ceilometer_sfcmet	✓	✓	✓			9	9
radiometer_ceilometer_sfcmet	✓	✓	✓	✓		67	97
radiometer_sfcmet	✓	✓		✓		65	96
sfcmet	✓	✓				7	8
windProfiler_ceilometer_sfcmet	✓	✓	✓		✓	46	31
windProfiler_radiometer_ceilometer	✓		✓	✓	✓	101	115
windProfiler_radiometer_ ceilometer_sfcmet	✓	✓	✓	✓	✓	104	119
windProfiler_radiometer_sfcmet	✓	✓		✓	✓	102	118
windProfiler_sfcmet	✓	✓			✓	44	30

The term "sfcmet" indicates that surface meteorological data were included in the scenario.

Source: Sonoma Technology, Inc., 2022.

A feature is defined as a measurable property from the data to be analyzed; they are typically the columns in a data matrix (the rows typically represent data at specific times). In the language of machine learning, a feature is an input variable to the ML algorithm and is distinct from other inputs such as hyperparameters. The number of features in the data for the different scenarios for Fremont and LAX are shown. Although it is possible to train a model using all available features, it is unlikely that all features contribute to meaningful predictions. Removing extraneous features can substantially speed model training and prediction without adversely impacting model accuracy. Removing extraneous features also help to prevent overfitting. To select variables, a preliminary XGBoost model was trained using all features and determined the importance of each input feature, retaining the top 30 percent of features based on their importance. Only the retained features (up to 104 for Fremont and 119 for LAX) were used for hyperparameter tuning and model training. This step was performed in

each round of model development. There were fewer features in Fremont because a sodar was not installed at that site (LAX had sodar and radar wind profiler data).

Solar Forecast Performance Analysis

In the solar forecasting community, numerous works have been devoted to the development of models that generate point forecasts also called deterministic forecasts. Standard metrics of deterministic forecast skill include Mean Absolute Error (MAE), Root Mean Square Error (RMSE), and Mean Absolute Percentage Error (MAPE). As renewable generation forecasts have become more deeply ingrained in electrical grid management algorithms probabilistic forecasts, which assign a probability to each of a number of different outcomes, have become increasingly valuable, and metrics of probabilistic forecast skill such as the Brier Skill Score are increasingly common. In this report, however, the project team only considers the deterministic metrics to evaluate performance of solar power forecasts with different models. The equations of the solar power forecasting evaluation metrics are shown in Appendix D.

Description of Method

The method adopted uses the metrics described in Appendix C to evaluate the performance of solar forecasting with Weather Research and Forecasting model data assimilation (WRFDA). The project team compared the solar forecasting results with and without WRFDA. In addition, the solar forecasting results obtained from the High-Resolution Rapid Refresh (HRRR) model were used as the benchmark.

Description of Data

This project aimed to evaluate solar power forecasting performance in areas under the California ISO's purview. The evaluation process could be conducted at three different levels: the resource level; the zonal level; and the whole-system level. The resource level analysis, however, was not allowed here, since the California ISO does not disclose the information at the individual resource level. The zonal level analysis could lead to better evaluation results than the system level analysis, but it has more requirements on data availability. Since it is difficult to obtain the geographical information of each individual solar resource from California ISO, it is not possible to map the resources to the zones for calculating the zonal solar forecasting values. Thus, the system level solar forecasting was the best choice for this project.

The benchmarking analysis in this section was based on the following dataset:

- *Actual solar forecasting data for California ISO*. The California ISO published actual solar generation in the system on its public Open Access Same-time Information System (OASIS) site (CAISO OASIS, 2019). The data is with 15-minute resolution. The data listed in CAISO OASIS contains two parts: actual solar generation in the system, and system-wide solar curtailment. In this study, the two parts were summed up to obtain the total solar power generation of California ISO at each 15 minutes.
- *System-wide solar forecasting with HRRR method*. As a control forecast, the project team used output from the US National Center for Environmental Prediction's High Resolution Rapid Refresh Analysis and Forecast System (HRRR) model. The HRRR model is a NOAA real-time, 3-km resolution, hourly updated, cloud-resolving, convection-allowing, atmospheric model, initialized by 3 km grids with 3 km radar

assimilation (NOAA, 2019). HRRR forecasts of global horizontal irradiance, interpolated to the locations of all solar generation stations in California ISO, were scaled by clear-sky radiance derived from the PVLIB python code library. The resulting fraction of clear-sky radiation was multiplied by the clear-sky generation of each station derived from station generation data by UL/AWS Truepower, which also supplied the archived HRRR data, and performed these calculations.

- *System-wide solar forecasting using the WRF model*. Data were provided by UL/AWS Truepower from runs of the eWRF model in the configuration developed to best model valley fog and marine boundary layer clouds in California. First, the forecasts of Global Horizontal Irradiance (GHI) for the 383 solar generating stations were obtained. The forecasts were initialized using three-dimensional height, temperature, water vapor, and cloud water fields as well as surface data for the 10 UTC run of the HRRR model each morning, run for at most 18 hours. The forecast lead time is T minus 10 hours where T is the time of day each day in hours UTC. The GHI forecast from the WRF model with Data Assimilation (DA) were then processed in the same way as the HRRR GHI predictions described above to yield solar generation forecasts. Finally, the forecasts on each station were summed up to obtain the system-wide solar forecast.
- *System-wide solar forecasting with WRFDA method*. Data were provided by UL/AWS Truepower from runs of the WRF model, as described above, with the WRF Data Assimilation (WRFDA) module turned on, to incorporate surface-based observations from Sonoma Technology, Inc. in the model runs.

The quality of the input data significantly impacts the evaluation results. It was observed that the received time-series included missing data and invalid data. The intervals with missing data and invalid data were eliminated in the below analyses.

Solar Forecast Value Assessment

As solar electricity penetration in the electric grid is increasing, the power generated by solar resources needs to be taken into account in the planning and operations of ISOs, balancing authorities and utilities. Solar forecasting is necessary for the economically optimal dispatch of generation resources and reliable operation of the power systems. However, there is still lack of clarity in the industry regarding the quantified value of solar power forecasting. The methods used to quantify the value of improved solar forecasting accuracy for electric utilities and grid operators are described in this section. One proposed method is to analyze the historical operation data from California ISO and use linear regression to identify correlations between improved solar forecasting accuracy and several metrics of grid operational efficiency including California ISO load payment, solar curtailment, and cleared reserve quantities. The other proposed method is to conduct production cost modeling (PCM) simulations on representative test systems. The outcome of PCM simulations would include change of system operation costs, change of balancing violations, and change of reserve violations.

Quantifying the Value of Improved Forecast Performance

Historical Data for Determining the Value of Improved Forecasting to Grid Operations

This analysis focused on identifying the potential value of forecast improvements to grid operations using proxy data based on recent conditions. The team examined and used recent historical data, such as prices and costs of energy and ancillary services, solar curtailment, and other operational metrics to understand the marginal improvement due to the improved forecasts.

The value of improved forecasts has two components. First, when forecasts improve, decisions based on those forecasts should produce benefits to the system operator, utility, and ratepayers. For example, if a forecast of high solar generation results in a low price offered to generators in the day-ahead market, and solar generation is in fact low, the power required to meet demand would have to be purchased at a later time from operating reserves and would be more expensive than if the forecast had correctly called for low solar generation. Second, when forecasts improve, and are known by their users to have improved, measures taken to hedge risks in case of forecast failure can be relaxed. Reducing reserve requirements, for example, can reduce costs. The latter source of savings depends on an accurate assessment of the distribution of forecast errors. If the skill improvement is smaller than anticipated, reserve margins may be set too low, resulting in more expensive power purchased late in the cycle.

The first component forecast value can be estimated using the historical record of forecasts, prices, and operating reserve margins. However, the second component can only be directly estimated when forecasts are presented in probabilistic form, and probabilities are calculated to take into account the impact of changing weather patterns on expected forecast skill. In that case, natural experiments, resulting from day-to-day changes in expected forecast skill, can be exploited to estimate how operators respond to changing expectations of forecast skill.

The research team developed a methodology to show the value of an improved forecast by time of day and under specific conditions noted by stakeholders as particularly important. Conditions that have been identified include peak and minimum load periods, ramping conditions, and other periods when the system, or a location on the system, may be constrained. For example, improved forecasting may reduce the need to call on operating reserves, which may both reduce costs (due to lowered reserve procurement) or improve reliability (due to reduced area control error). The analysis used one year of historical system data for the calculations and developed a spreadsheet that stakeholders can continue to update and use to evaluate the value of the forecast improvements after project completion. The research team conducted utility-specific forecasting evaluations by quantifying the value of forecasting on specific days or day types (e.g., holidays, weekdays, or weekends), which are defined by each utility. A marginal cost approach is taken, where it can be assumed that improvement in economic efficiency can be approximated using the marginal prices or operating reserves reduction valued using the price of reserves in the hours for which reduction occurs. Similarly, for utility transmission and distribution operations, the value of reduced wear and tear on equipment or solar curtailment is quantified on the basis of recent experience.

Table 10 shows the metrics proposed for assessing the values of improved solar forecasting, which includes both economic and grid reliability values and uses historical data from the utility and California ISO. The study assesses the economic value directly from system LMP and ancillary services data, without having to make detailed production cost simulations. The

evaluation of reliability value is based on those metrics beyond market operations, such as improved voltage management at feeder, improved load forecasting, impacts on outage schedule, and electric heat interaction.

Table 10: Proposed Metrics to Measure the Value of Improved Solar Power Forecasting

Type	Metrics
Economic Value (By time of day and under specific conditions noted by stakeholders)	Cost Savings
	Reserve Reduction
	Curtailment Reduction
	Value of reduced wear and tear on equipment
Grid Reliability Value	Improved voltage management at feeder (distribution level)
	Frequency performance/voltage on the bulk system (transmission level)
	How improved BTM solar forecasting improves the peak demand forecasting accuracy
	Impacts on outage schedule
	Electric heat interaction

Source: Electric Power Research Institute, 2022.

Use of Production Cost Models to Analyze the Value of Solar Forecast Improvements

High solar PV penetrations are likely to be significantly impacted by phenomena such as marine layer and fog. To understand the value of forecast improvements, detailed simulations of how the system will operate must be performed. Production simulation models have typically been used to simulate power system operations with and without improved forecasting methods, in order to understand potential value. Using advanced production simulations, the same values identified (energy efficiency, reliability, etc.) can also be calculated for future conditions.

EPRI has implemented the production cost simulation tool—Power System Optimizer (PSO) by Polaris Systems Optimization—in many studies. The PSO was used to simulate the multi-timescale unit commitment (UC) and economic dispatch process for calculating the benefits attributable to improved solar forecasting accuracy. The simulation process mimics the actual operation of California ISO grid operations staff. However, due to the lack of a detailed network model of the California ISO system, the project team conducted the studies on two existing public test systems and modified the generation mix to represent the California ISO. The two systems were the National Renewable Energy Laboratory Reliability Test System (NREL-RTS) (Preston, E. and Barrows, C., 2018), and a reduced-form Western Electricity Coordinating Council (WECC) system with 240 buses (Price, J. et al., 2011). The framework for conducting the production cost simulations is shown in Figure 7.

Figure 7: Production Cost Simulation Framework

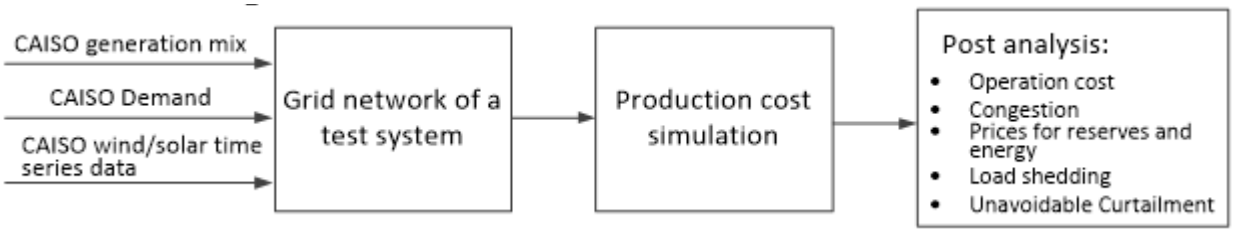

Source: Electric Power Research Institute, 2022.

The metrics shown in Table 10 can still be applied to evaluate the value of solar forecasting improvements. Instead of deriving the values of the metrics from historical data, this approach calculates those values from the results of production cost simulation. By simulating the test systems with and without including solar forecasting improvements, PSO can calculate the changes of operating cost, reserve, curtailment, and LMP.

For the historical data analysis (not using the production cost modeling), a spreadsheet-based analysis was developed to calculate the various value streams. This was first developed using a subset of the overall data (such as one month of data) so that the analysis could be tested and improved throughout the final year of the project. Then it was completed and used in the final analysis for quantifying the project benefits.

The commercial production cost simulation software PSO (PSO, 2019) was used for this study. PSO supports the modeling of multi-level, nested time intervals that simultaneously optimize energy and ancillary services. In this session, there are two cycles for all the simulations in PSO: the day-ahead (DA) cycle, which runs the unit commitment model on an hourly basis for the next day; and the real-time (RT) cycle, which commits the fast-start units and determines the dispatch results of all resources on a 5-minute basis.

The production cost simulation was run for the original case first. Then the project team conducted a solar forecast improvement scenario run, where the original solar forecasting data was replaced by the improved solar forecasting data. By comparing the results between the two runs, the benefits of solar power forecasting improvement could be obtained.

In this study, the project team assumed that the solar power forecasting was uniformly improved at all time horizons. The method is illustrated in Figure 8. Assuming the actual solar generation at time t is x_0, and the original solar forecasting at time t is x_1, the forecast error at t is x_1-x_0. When the solar forecast was improved by 20 percent, the forecast error was reduced to 0.8*(x_1-x_0). The improved DA solar forecast value x_2 was calculated as 0.8*(x_1-x_0) + x_0. The process was repeated for all simulated intervals to get the solar power forecast improvement time-series profile. A better way to obtain the improved solar forecasting data, though, would have been based on the field data through the RF-Solar data initialization experiments from Sonoma Technology, Inc. and UL Renewables. This might be difficult because the meteorological sensors are only located in limited places, and information for individua PV sites is not allowed to be shared.

Figure 8: Soar Power Forecasting Improvement Method

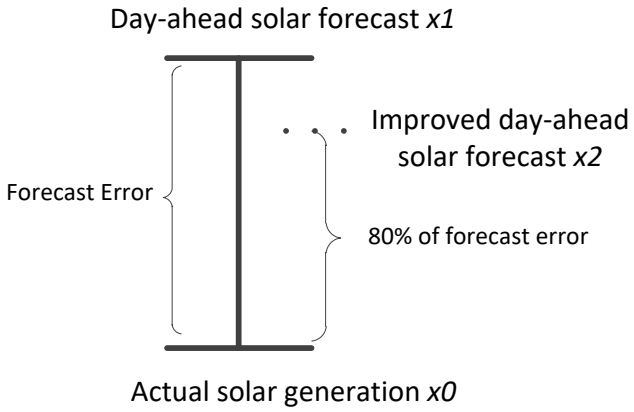

Source: Electric Power Research Institute, 2022.

Grid Impacts Assessment of Improved Solar Forecasting Versus Energy Storage Resource

As solar energy becomes a bigger part in the generation mix of power systems, new challenges with regard to grid integration of solar power are emerging. Improved solar forecasting could increase grid operation flexibility, reduce operation uncertainty, and give grid operators better visibility regarding how much solar power will be generated in the near future. These benefits enable the electric power grid to adapt to changing conditions in a better manner, and eventually lead to lower system operation cost and reduced electricity supply disruptions.

In this section, the grid impacts of improved solar forecasting and energy storage resources are evaluated. The impacts are measured by two metrics: the economic metric represented by the system's production cost and the reliability metric represented by the quantity of energy violations to balance the generation and demand.

The procedure to quantify the benefits of improved solar forecasting versus battery storage is as follows:

- Step 1: Create a *Base Case* with representative hourly load shape and projected generation resources in the system. The fuel cost, thermal unit startup cost and balancing violations are calculated for the *Base Case*.
- Step 2: Improve the day-ahead solar forecasting by *x* percent on the Base Case and rerun the production cost model. This leads to the *Solar Forecast Improvement Case*.
- Step 3: Add *y* MW battery storage to the *Base Case* and rerun the production cost model. This leads to the *Additional Battery Storage Case*.
- Step 4: Run numerous sensitivity studies by changing the y value. Calculate the fuel cost, thermal unit startup cost and balancing violations in each study. Select the case study that has similar cost and reliability benefits as the Solar Forecast Improvement Case. The y value under this case is the battery storage capacity needed in the system to achieve same-size benefits as x percent solar forecast improvement in the day-ahead.

CHAPTER 3:
Project Results

This chapter summarizes the key results of the following technical topics: (1) field data collection program, (2) physical and statistical prediction modeling, (3) machine learning for very short-term predictions, (4) solar forecast performance analysis, (5) solar forecast value assessment, and (6) grid impacts assessment of improved solar forecasting versus energy storage resource. The key results for each topic are summarized, while more detailed results are shown in the appendices.

Summary of the Results from Field Data Collection Program

One of the challenges in this measurement program was suitably locating Sodar and RASS instrumentation. Because sodar and RASS instruments produce significant audible noise (~ 90-95 dbA), they must be located away from residences and businesses to avoid noise nuisance. In some cases, it may not be possible to site these instruments in parts of urban areas where they could provide the most benefits for solar energy forecasting needs. For example, the RASS was installed at the Fremont core site for this study but was turned off after the first week due to noise complaints (the nearest residences were about 500 feet from the instrument).

Instrument breakdowns can also affect data collection for any field measurement project. The profiling instruments used in this project have proven to be reliable instruments for meeting long-term energy forecasting needs and objectives (Wilczak et al., 2015, 2019), and most instruments performed well throughout the measurement period (as shown by the high data completion rates in Appendix A, Table A-1). The microwave radiometer that was planned for collecting measurements in winter fog conditions at the Visalia core site failed unexpectedly after it was deployed. After repairs were completed, the radiometer was successfully used at the Fremont core site, as planned, to collect measurements in marine stratus conditions in the San Francisco Bay Area. The same radiometer was re-deployed to the Bruceville/Sacramento supplemental site in December 2018 to collect additional data during radiation fog conditions. An added challenge for this project was that many of the instruments were not owned, operated, or maintained by the project team. As an example, the RWP instruments became inoperable after September 2018 at the LAX and Irvine core sites; fortunately, these failures occurred after the bulk of the marine stratus season in southern California.

There were far more days of coastal marine stratus compared to inland radiation fog during the measurement period. This is climatologically normal, but concurrent changes in air pollution, agricultural burning, and climate may reduce the number of fog days in the Central Valley over time (Baldocchi and Waller, 2014). The winter of 2017/2018 was preceded by exceptional drought throughout California, which reduced the soil moisture and boundary layer humidity needed to form radiation fog despite otherwise ideal weather conditions. The field deployment did not begin until late December 2017, but there were no significant radiation fog events in the Central Valley until mid-January 2018. In February 2018, an active storm pattern in California limited the number of radiation fog events in the Central Valley. The limited number of radiation fog cases was problematic for developing statistical forecasting

approaches, as supervised machine learning approaches require substantial historical training data. Forecasting inland radiation fog formation and dissipation remains an important challenge for NWP models and for forecasting solar radiation. Long-term boundary layer profile measurements are needed to increase the number of radiation fog cases available for future model evaluation and improvements.

Physical and Statistical Prediction Modeling

Sensitivity Experiment Data and Results

The goal of research activities in this technical area was to perform experiments that evaluate the sensitivity of intra-day (0-24 hours) WRF-Solar stratus and fog forecasts for a range of key physical parameters embedded in the physics sub-models. Sensitivity was performed on a sample of approximately ten marine layer stratus and fog cases and approximately ten radiation stratus and fog cases.

The baseline configuration of the WRF model for these experiments consisted of the RRTM long- and short-wave radiation scheme; the Thompson Aerosol-Aware microphysics scheme (using climatological aerosol concentrations), with radiation scheme calls every 5 minutes; the Noah land-surface model with nine surface layers; the Kain-Fritch cumulus scheme, called every 5 minutes; and the Yonsei University (YSU) boundary layer scheme, with top-down mixing option turned on. This set-up was designed to approximate the WRF-Solar configuration (Thompson Aerosol-Aware microphsyics, frequent radiation calls); top-down mixing was turned on following the work of Wilson and Fovell (2017) who developed this modification to improve the representation of fog layers in the California Central Valley.

The sensitivity experiments varied both radiation and boundary layer schemes to test the dependence of results on these parameterization choices. These experiments are summarized in Table 11. Experiments were performed for the months of January, August and September 2018. Results from January are presented in this report because the results from other months did not significantly alter the conclusions drawn from the January results.

Table 11: Experiment Names and Descriptions

Experiment	Description
Baseline	RRTM Radiation & YSU Boundary Layer with Top-Down Mixing
MYJ Boundary Layer	RRTM Radiation, MYJ Boundary Layer
Grenier Boundary Layer	RRTM Radiation, Grenier Boundary Layer
YSU Top-Down Mixing Off	RRTM Radiation, YSU *without* Top-Down Mixing
RRTMG Radiation Scheme	RRTMG Radiation, YSU with Top-Down Mixing

Source: UL Renewables/AWS Truepower, 2022.

January 2018 presented a rich variety of weather scenarios in California. Figure 9 shows noon-time satellite imagery, taken in the red-light channel (channel 2) by the GOES 16 geostationary satellite imager. Red colors indicate low values of reflectivity, while yellows, greens, and blue indicate successively high values of reflectivity. For example, on January 13, the Central Valley can be seen to be largely filled by a thick and highly reflective cloud layer, while on January 20th, only a small amount of low cloud is present in the southeastern edge of the Valley. There are nearly clear days as well (such as January 27) and overcast days with

no fog (for example January 2). Figure 9 (using the same color scheme as Figure B-3) shows time series of the fraction of the Central Valley with boundary layer clouds present in each model run, and the fraction of the Central Valley with reflectivity greater than 30 percent of the maximum reflectivity value.

Figure 9: Boundary-Layer (below the 850 hPa level) Cloud Fraction Averaged over the Central Valley of California - January 11, 2018

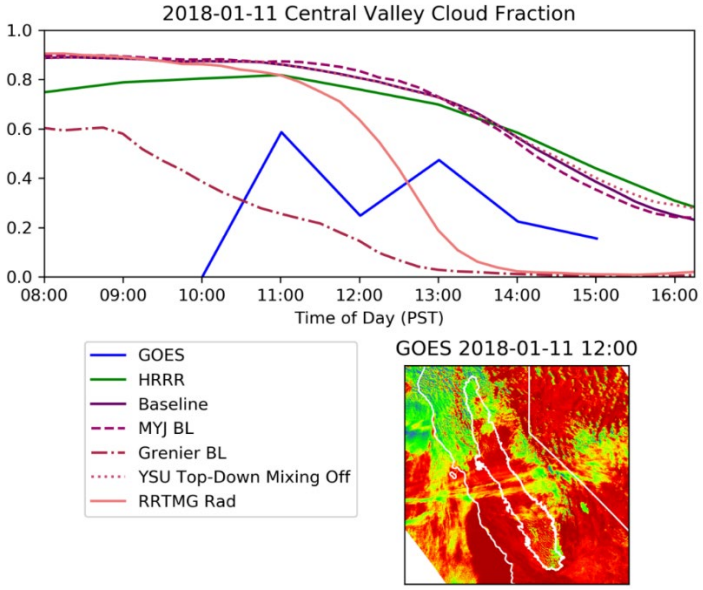

Source: UL Renewables/AWS Truepower, 2022.

A consistent pattern emerged from the sensitivity experiment results. Little sensitivity to the top-down mixing parameterization in the YSU boundary layer scheme was observed This parameterization enables additional mixing of dry air from above the boundary layer into boundary clouds, which should result in quicker break-up of fog layers. The experiment results confirm this tendency, but the difference in resulting cloud fraction and time of break-up is small. Turning the top-down mixing off results in a few percent increase in Central Valley cloud fraction towards the end of the day. Replacing the YSU boundary scheme completely with the Mellor-Yamada-Janjić (MYJ; Janjić, 1994) scheme also results in a slight increase in early-day boundary cloud and a slight reduction in late-day boundary cloud. However, the two other changes result in much more dramatic changes.

Replacing the YSU scheme with the Grenier-Bretherton-McCaa Boundary Layer scheme (Grenier et al., 2001; Bretherton et al., 2004), which was designed in particular to simulate cloud-topped boundary layers, resulted in a dramatically earlier break-down of boundary layer cloud, especially after sunrise, in all cases. Similarly, but less dramatically, replacing the RRTM radiation scheme with the Rapid Radiative Transfer Model used in the Global Forecast System (RRTMG) radiation scheme (Iacono et al., 2008) results in much more rapid break-up of the Central Valley boundary layer clouds, starting around 11 am each day. The RRTMG scheme includes several features designed to improve handling of sub-grid-scale cloudiness but is largely intended to simply speed calculations with respect to the RRTM scheme while maintaining accuracy (Iacono et al., 2008), so this strong sensitivity is unexpected. In most cases, the HRRR results tracked those from the baseline WRF set-up, but in a few cases (for

example January 27, when actual cloud cover was much more limited than any of the model runs) the HRRR tracked closer to the RRTMG results.

To gain additional insight into the differences in cloud behavior in the various runs, Figure 10 shows vertical profiles of cloud cover throughout the model runs from 2 am (blue) through 8 pm (purple) at four locations around California (Visalia denoted as VIS, Irvine denoted as IRV, Los Angeles Airport denoted as LAX, and Whiteman Airport denoted as WHP). The figure shows that the Grenier scheme has dramatically lower cloud water mixing ratios in almost all cases, even where clouds are present. It was outside the scope of this study to diagnose the reasons for this phenomenon, but it should be noted for future consideration that the Grenier scheme maintains ground fog in some cases when clouds aloft are lost. This scheme is clearly ruled out as an outlier.

The contrasts in cloud water profiles in the RRTMG experiment are more subtly different from the WRF baseline case. The results for January 13 is a representative example. Throughout the morning, the baseline and RRTMG cases show a similar lowering of the cloud tops and reduction in cloud water near the surface; however, after local noon, there is a sudden disappearance of cloud. This suggests that the radiative scheme is handling cloud variability very differently in the RRTMG: once cloud water mixing ratio goes below a threshold, radiation may be allowed to penetrate much more easily to the surface, warming it, and driving convective warming of the boundary layer that results in rapid evaporation of the remaining cloud water.

Figure 10: Profiles of Cloud Water Mixing Ratio (in ppm) at Four Locations

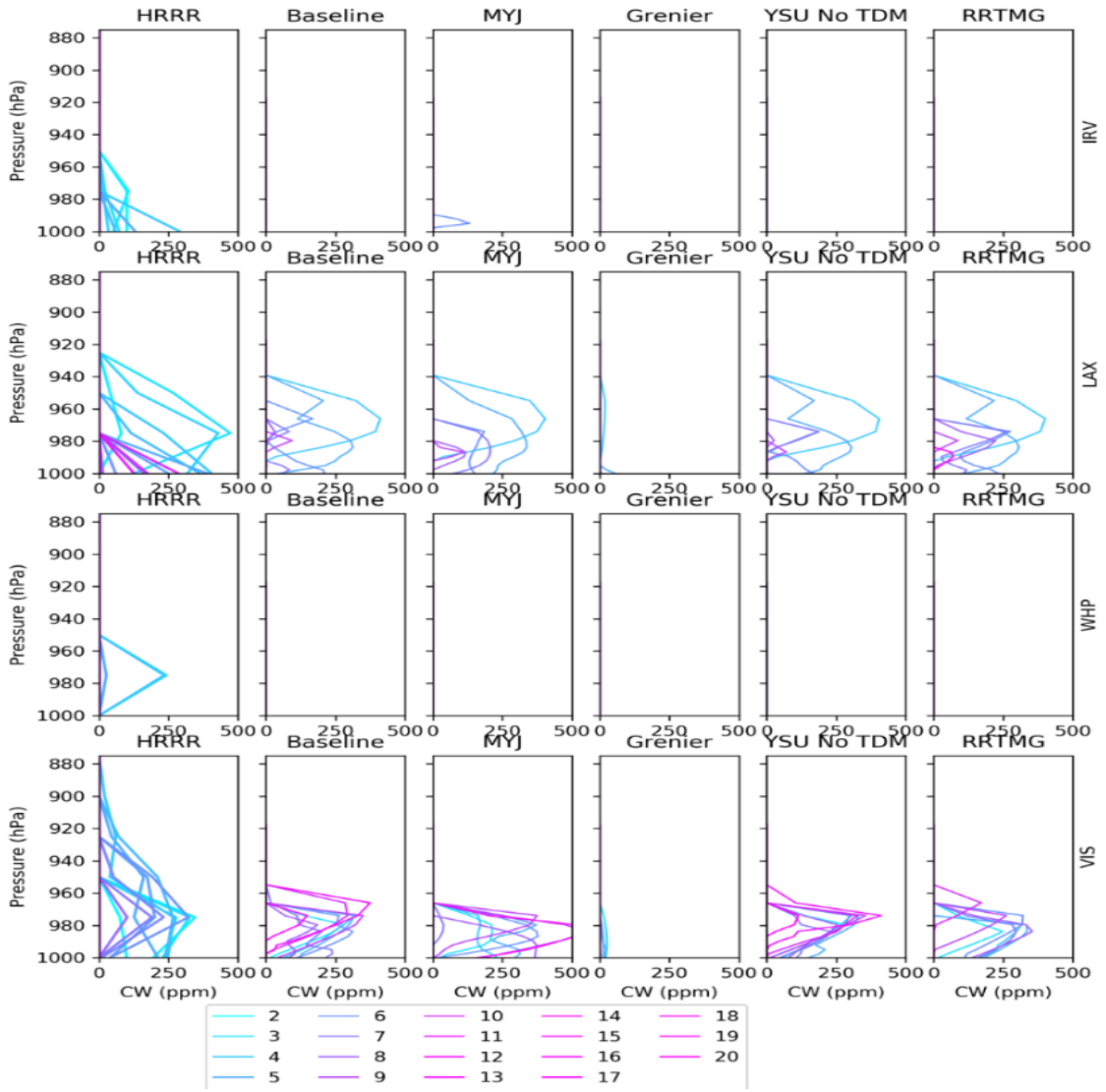

From top to bottom, Irvine, Los Angeles Airport, Whiteman Airport, and Visalia, and for the HRRR (left column) and the Baseline, MYJ, Grenier, YSU w/o Top-Down Mixing, and RRTMG WRF experiments, on January 7, 2018. Color Indicates Time of Day, from 2 am to 8 pm (labeled 20).

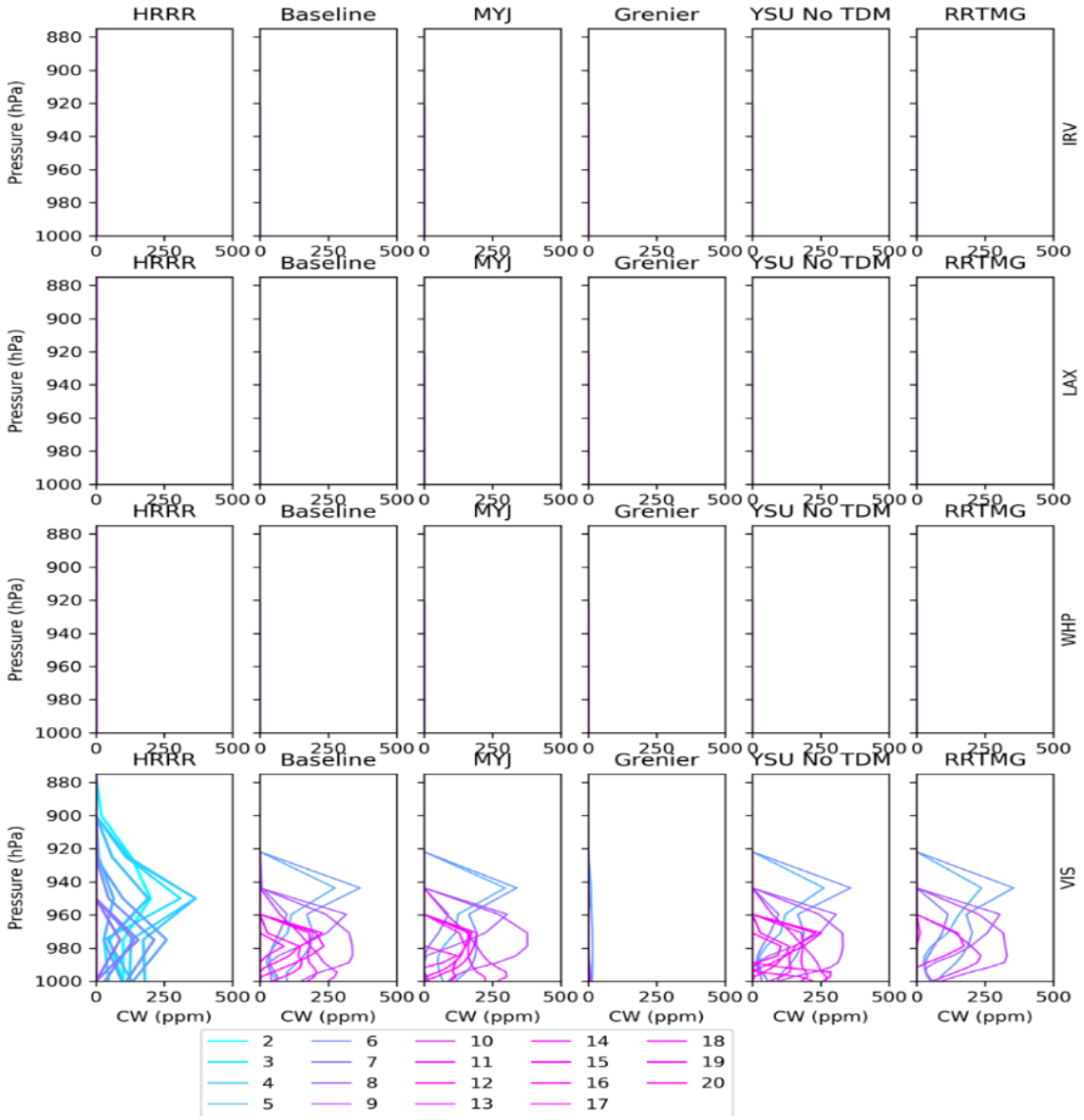

From top to bottom, Irvine, Los Angeles Airport, Whiteman Airport, and Visalia, and for the HRRR (left column) and the Baseline, MYJ, Grenier, YSU w/o Top-Down Mixing, and RRTMG WRF experiments, on January 13, 2018. Color Indicates Time of Day, from 2 am to 8 pm (labeled 20).

Source: UL Renewables/AWS Truepower, 2022.

the

The results presented in this section show clear biases among the different sensitivity experiments. However, while they appear to conclusively rule out the Grenier scheme as producing unrealistically dry model boundary layers, they do not strongly favor any of the remaining choices. The cases of January 11 and 12 demonstrate that rapid break-up of Central Valley fog in the afternoon does occur with some frequency, and the RRTMG scheme seems to be better able to reproduce this behavior. Because these results do not conclusively show that one radiation and boundary layer set up is superior to all others, sensitivity experiments were repeated in the context of a full data-assimilation system. This was done to show how these schemes influence model behavior when additional local information on initial conditions (beyond those available to HRRR) are available. These experiments are discussed in the section on data assimilation.

Several pathways towards improved use and evaluation of data assimilation to increase the accuracy of Central Valley and Coastal fog and low-cloud forecasting are available for use in future WRFDA model runs:

- Forecast runs covering the month of September 2018, when many episodes of coastal fog were observed, will be run.
- Extraction of point forecasts of global horizontal irradiance at locations where this is measured, and at locations where solar generation is known will be performed to evaluate forecast skill changes due to data assimilation more comprehensively.
- Additional experiments with the assumed model variance and covariance length scales could be performed, that might lead to improved matches of forecasts with observations.
- Rather than using the pre-defined error covariance option in WRFDA 3DVAR, it is also possible to use co-variances obtained from preceding model runs. This process requires about a month of pre-existing forecasts, and so would involve running the WRF model for the month of December 2017 to generate co-variances for January 2018 runs, then running from January 2018 forward using data assimilation and updating the co-variances from each previous month.

Rather than using the 3DVAR approach, more advanced WRFDA 4DVAR could be used, which involves a process of running a simplified WRF model backwards and forwards in time to increase the physical consistency of the atmospheric state while bringing it as close as possible to the observed conditions. This option appears in initial tests to require greater computational power than UL's facilities would allow in real-time operation, but improved procedures might make it possible.

Machine Learning for Very Short-Term Predictions

The project team conducted a preliminary analysis using both the RF and XGBoost algorithms to predict both cloudiness and solar radiation at Fremont, with different time lags applied to evaluate forecast skill at different forecast horizons ranging from 15 minutes to 2 hours. The preliminary analysis used only the binary cloud classification (Classes 0 [Clear] and 3 [Stratus]) and excluded data from the Fremont radar wind profiler data.

Table 12 and Table 13 summarize the model performance statistics for predicting cloudiness and solar irradiance at Fremont, while Figure 11 shows comparisons between the predicted and observed solar irradiance at the 0- and 1-hour forecast horizons.

Table 12: Model Performance Statistics for Binary Cloud Cover from Random Forest and XGBoost Models at Fremont

	Random Forest			XGBoost		
Forecast horizon (mins)	**Accuracy (%)**	**Sensitivity (%)**	**Specificity (%)**	**Accuracy (%)**	**Sensitivity (%)**	**Specificity (%)**
0	99.4	96.9	100.0	100	100	100
15	97.3	89.7	99.1	97.5	93.6	98.4
30	96.6	86.7	98.8	97.4	91.7	98.6
45	96.8	86.9	99.1	97.0	90.5	98.5
60	95.9	83.8	98.5	96.7	89.0	98.4

Source: Sonoma Technology, Inc., 2022

The 0-hour forecast horizon is not a forecast but is shown as a baseline reference. For cloud cover predictions, the XGBoost model performed slightly better than the RF model in terms of accuracy and sensitivity. Both models performed with accuracy greater than 95 percent for forecast horizons of up to 1 hour. For solar irradiance predictions, the XGBoost model also performed slightly better than the RF model. The correlation coefficient was similar between the two models, but the RMSE for the XGBoost model was smaller for 1-hour cloud forecasts. Note that the performance statistics shown were based on the test dataset. Since the performance statistics are not significantly different from the performance statistics for the training set (data not shown), there is a low probability of overfitting. The preliminary performance results were encouraging and supported continued work to refine the models and approach. Because the XGBoost model performed better than the RF model, subsequent discussion focuses on results from the XGBoost model.

Table 13: Model Performance Statistics for Solar Irradiance from Random Forest and XGBoost Models at Fremont

	Random Forest		XGBoost	
Forecast horizon (mins)	R^2	RMSE (W/m^2)	R^2	RMSE (W/m^2)
0	0.94	68.1	0.95	65.5
15	0.95	65.8	0.95	67.1
30	0.94	70.7	0.94	68.4
45	0.95	68.0	0.94	70.6
60	0.94	72.3	0.94	69.2

Source: Sonoma Technology, Inc., 2022

Figure 11: Observed and Predicted Solar Irradiance (W/m^2) at Fremont.

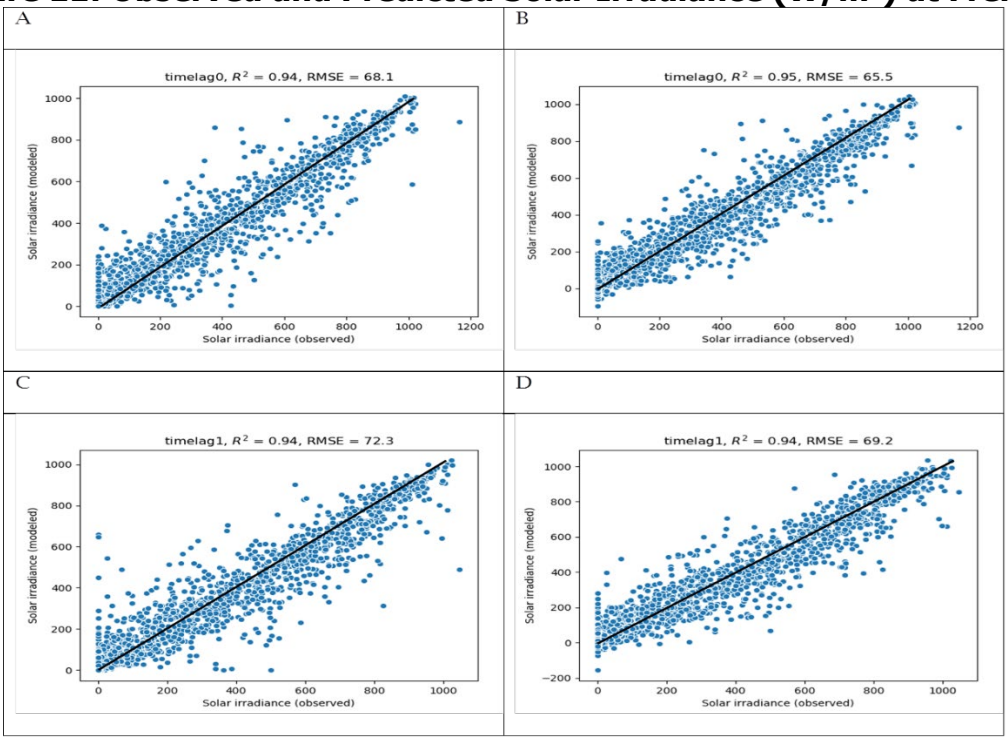

Solar Irradiance is shown for A) the RF Model with no time lag; B) the XGBoost model with no time lag; C) the RF model for a 1-hour forecast horizon; and D) the XGBoost model for a 1-hour forecast horizon.

Source: Sonoma Technology, Inc., 2022

The project team evaluated the preliminary XGBoost model for Fremont for several forecast horizons (time lags) ranging from 15 minutes to 4 hours and compared the results to a persistence forecast. Persistence (specifically the forecast is the same as the current state) is a rudimentary but useful baseline model that provides context for assessing ML model performance. At a minimum, a useful model should provide predictive skill that exceeds that of a persistence model.

Table 14 shows the performance of the XGBoost and persistence models for predicting stratus clouds at Fremont for several time lags. For XGBoost, performance is best for all metrics at the 15-minute and 30-minute forecast horizons. Accuracy drops slightly at the 45-minute and 60-minute forecast horizons. At the 15-minute forecast horizon, the XGBoost forecast is no better than persistence. For forecast horizons beyond 15 minutes, the persistence forecasts degrade rapidly and the XGBoost model outperforms the persistence model.

Table 14: Model Performance Statistics for Cloud Cover from the XGBoost Model and the Persistence Model

Forecast Horizon (minutes)	0	15	30	45	60	120
XGBoost						
Accuracy (%)	100	97.7	97.5	96.5	97.2	97.0
Sensitivity (%)	100	93.8	90.7	88.8	90.2	87.3
Specificity (%)	100	98.5	99.0	98.1	98.6	99.1
Persistence						
Accuracy (%)	--	97.7	96.2	95.0	94.4	90.0
Sensitivity (%)	--	93.1	88.2	85.5	84.5	71.4
Specificity (%)	--	98.7	94.9	96.9	96.4	94.0

Source: Sonoma Technology, Inc., 2022

SHapley Additive exPlanations (SHAP) analysis (https://papers.nips.cc/paper/7062-a-unified-approach-to-interpreting-model-predictions.pdf) is used to interpret model predictions and identify important predictors in the ML forecasts. Figure 12 shows a summary plot of SHAP values for ML-based 1-hour forecasts of cloudiness from the XGBoost algorithm at Fremont. The figure shows SHAP values for several 20 different parameters (y axis) from the sensor data, ranked by importance in the ML algorithm. A positive SHAP value (x axis on the plots) represents the contribution to predicting a cloudy condition, and a negative SHAP value represents the contribution to predicting a clear-sky (i.e., cloud-free) condition. The colors in the SHAP plots represent the values of the predictors, with blue indicating a low value and red a high value.

From the SHAP analysis, the most important predictor is the cloud base height measured by the ceilometer (ceil_CLOUD_1). This is expected since the cloudiness condition was derived from the cloud base height. The other important predictors include hour of the day, solar irradiance, temperature, relative humidity, and water vapor mixing ratio measured near the surface and in the lower boundary layer (below 350 m agl).

In general, low solar irradiance, lower temperature, higher relative humidity, and higher water vapor mixing ratio lead to predictions of clouds by the models, and vice versa. These results are consistent with the conceptual model for fog and stratus formation and dissipation. These results also suggest that temperature and moisture profiles from the microwave radiometer may add value for predicting cloud cover at the Fremont site.

Figure 12: SHAP Values for the XGBoost Model for Predicting Cloudiness at Fremont with a 1-hour Forecast Horizon

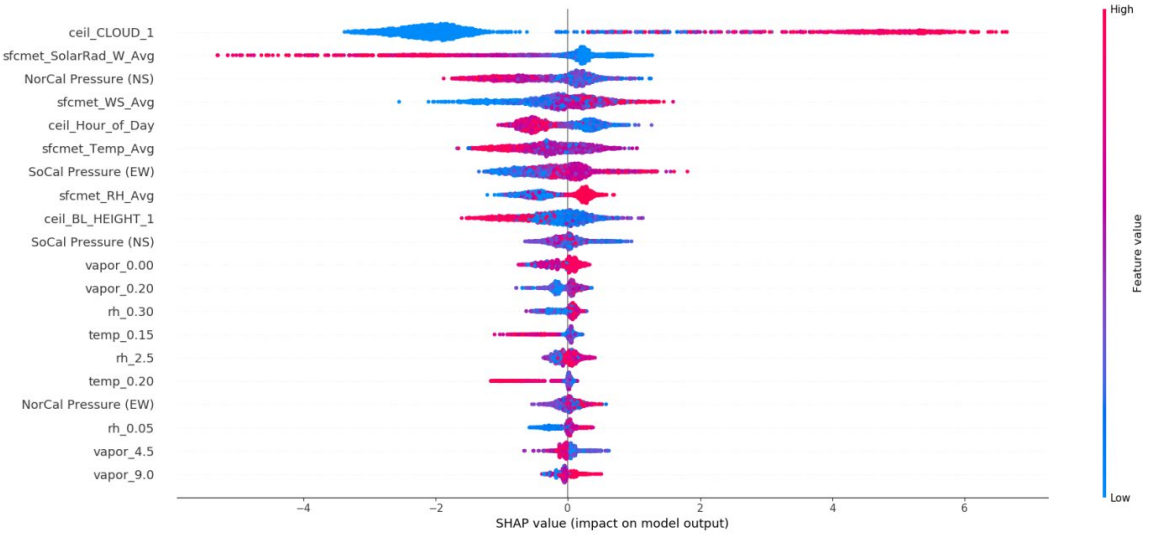

Source: Sonoma Technology, Inc., 2022

Figure 13 shows a summary plot of SHAP values for ML-based 1-hour forecasts of solar irradiance at Fremont. For the solar irradiance forecast models, the most important feature is hour of the day. Other important predictors include temperature and water vapor mixing ratio measured at the surface and in the lower atmosphere.

Figure 13: SHAP Values for the XGBoost Model for Predicting Solar Irradiance at Fremont with a 1-hour Forecast Horizon.

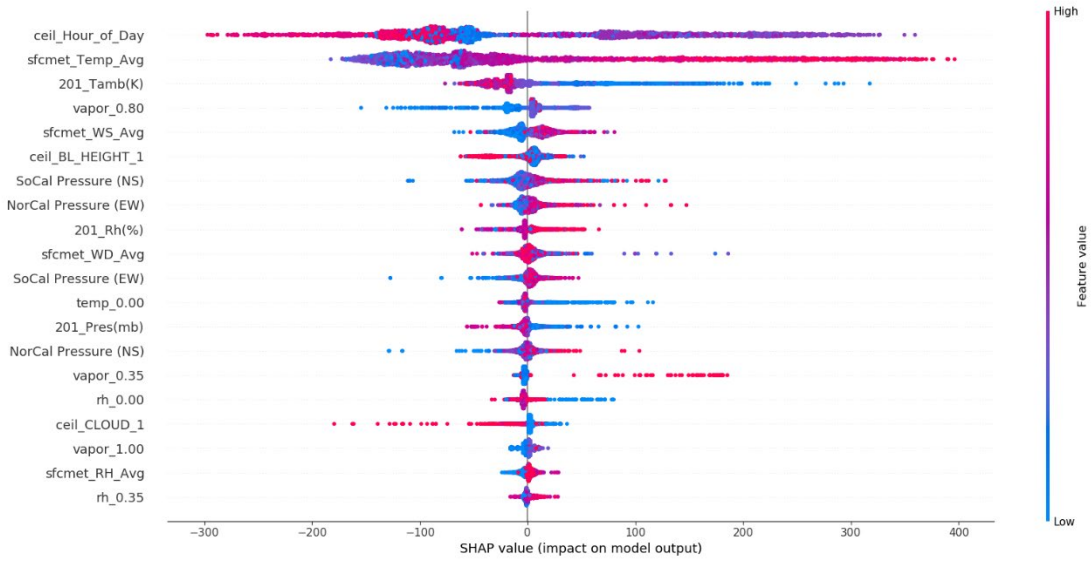

Source: Sonoma Technology, Inc., 2022

As with the cloud prediction models, these results suggest that radiometer data may add value for predicting solar irradiance at Fremont. Note that the SHAP analysis identified water vapor mixing ratio from the radiometer at 0.8 km and 0.9 km agl as important parameters; however,

these parameters are likely just noise and add no real value to the prediction given that high and low mixing ratios yielded positive and negative SHAP values (specifically unable to delineate the blue and red dots for this feature). The SHAP analysis provides valuable insights on selecting candidate predictors for refining the ML models.

Based on this preliminary analysis of results at the Fremont site, the ML models for both the RF and XGBoost algorithms yielded promising results at predicting cloudiness and solar irradiance for forecast horizons of up to 1 hour, with a forecast accuracy of greater than 95 percent (for cloud predictions) and a RMSE between 65 and 70 watts per square meter (W/m2 for solar irradiance predictions). The forecast performance was slightly better with the XGBoost algorithms, and the ML performance exceeded that of a persistence baseline forecast for forecast horizons greater than 15 minutes. Data from the microwave radiometer may add value for predicting cloud and solar irradiance at Fremont. Important predictors identified by a SHAP analysis included temperature, relative humidity, and water vapor mixing ratio measured in the lower boundary layer. The SHAP analysis showed that the relationships between these predictors were consistent with the conceptual model for fog and stratus formation and dissipation.

Based on results from the preliminary Fremont analysis, the project team refined and expanded the ML analysis to also include predictions for the LAX site. Since the XGBoost model performed slightly better than the Random Forest model, the refined analysis used the XGBoost algorithm. The project team used SHAP analysis to interpret model predictions and identify important predictors in the ML forecasts and conducted sensitivity experiments to assess which sensors and parameters provided the most value in improving cloud and solar irradiance forecasts. The detailed methodology and results of the refined analysis are shown in Appendix C. In summary, adding project sensor data to the machine learning models resulted in 4-23 percent improvement in cloud predictions compared to baseline machine learning models that only used routinely available synoptic meteorological data. The baseline model showed more skill at predicting stratus cloud and clear-sky conditions, and less skill at predicting transitions between stratus and clear-sky conditions. Models that included wind profiler data generally outperformed models that excluded wind profiler data, but the benefits of including radiometer data in the ML analysis were inconclusive.

Solar Forecast Performance Analysis

Mean Absolute Error

A comparison of Mean Absolute Error (MAE) values between hour 7 (7 am PST) and hour 17 (5 pm PST) for HRRR, WRFDA OFF, and WRFDA ON methods is shown in Figure 14. Between hour 7 and hour 9, the WRFDA ON curve has lower MAE values than the WRFDA OFF curve, indicating that the WRFDA method slightly improves the solar forecasting in the morning. However, in the afternoon hours, the WRFDA ON curve is above the WRFDA OFF curve, indicating that the WRFDA method does not improve the solar forecasting in the afternoon.

The limitation of improvements in the very early hours of the forecast can be understood by considering the limited physical range of the observations: within several hours of forecast initiation the information derived from improved initial conditions will in many cases have been advected away from the forecast area by the flow of wind in the atmosphere. After that time, any small errors in the initial conditions introduced in the data assimilation process may tend

to dominate over the improvement derived by bringing the initial conditions closer to observations in a few discrete locations. In the time-series curves in Appendix D, the project team did observe that the WRFDA ON curve has smaller forecasting error values than the WRFDA OFF curve in many intervals, but not all intervals in the year. It is expected that improved data assimilation processes will extend the usefulness of the data assimilation process by a few hours.

The improvements to the forecast derived from the WRF runs relative to the HRRR model that was used to initialize the WRF runs also exhaust themselves after about 10 am PST (18 UTC, eight hours into the WRF runs).This suggests that future work should focus on running the WRF model for only those first eight hours, beyond which improvements over the HRRR runs are unlikely. This would also save considerable computing power, making possible a larger ensemble of runs, or runs at higher resolution.

Figure 14: Mean Absolute Error of Solar Forecasts with Different Methods

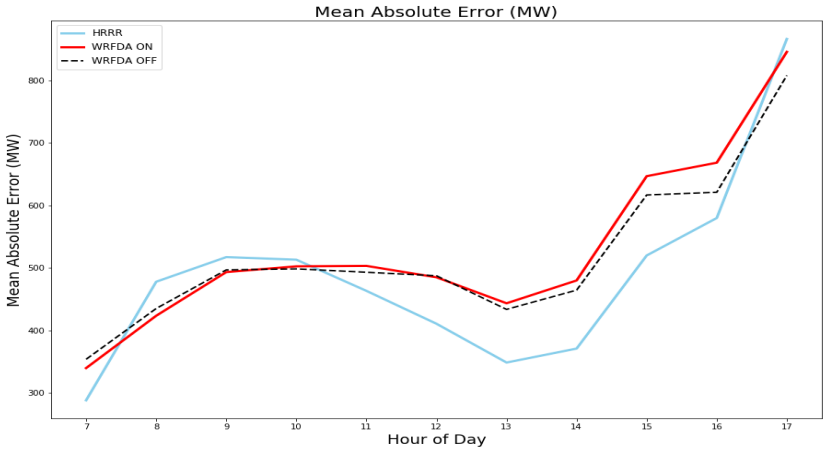

Source: Electric Power Research Institute, 2022.

Mean Absolute Percentage Error

The Mean Absolute Percentage Error (MAPE) curves for three methods are shown in Figure 1511. The percentage values were calculated based on an approximation of the installed solar power capacity in California ISO. The process for the approximation is as follows. First, the actual solar generation data for year 2018 was obtained from California ISO OASIS. The maximum instant solar generation was 12002 MW. Then it was assumed that the ratio of maximum solar generation to the installed solar power capacity was 80 percent, so. So that the total installed solar power capacity was 15010 MW.

Figure 15: Mean Absolute Percentage Error of Solar Forecasts with Different Methods

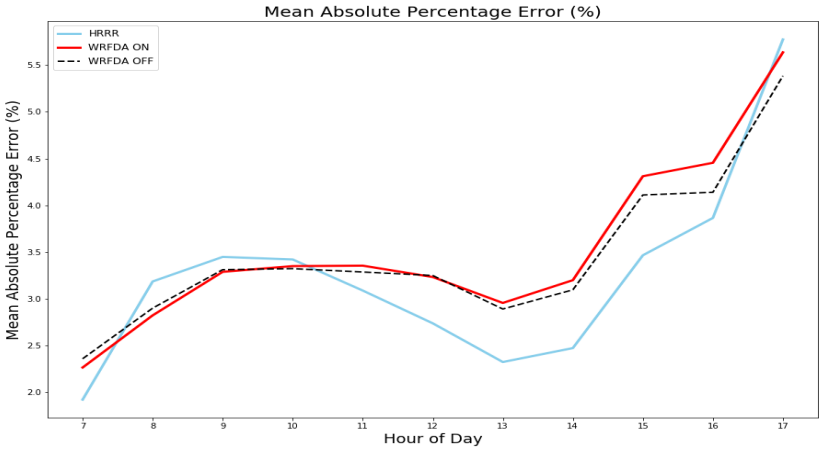

Source: Electric Power Research Institute, 2022.

Mean Bias Error

The Mean Bias Error (MBE) curves for the three methods are shown in Figure 16. Note that at hour 7 all three methods gave negative MBE values, meaning that the models tend to under-forecast at hour 7. For the rest of the hours, the MBE values are positive which means that the models tend to over-forecast in those hours.

Figure 16: Mean Bias Error of Solar Forecasts with Different Methods

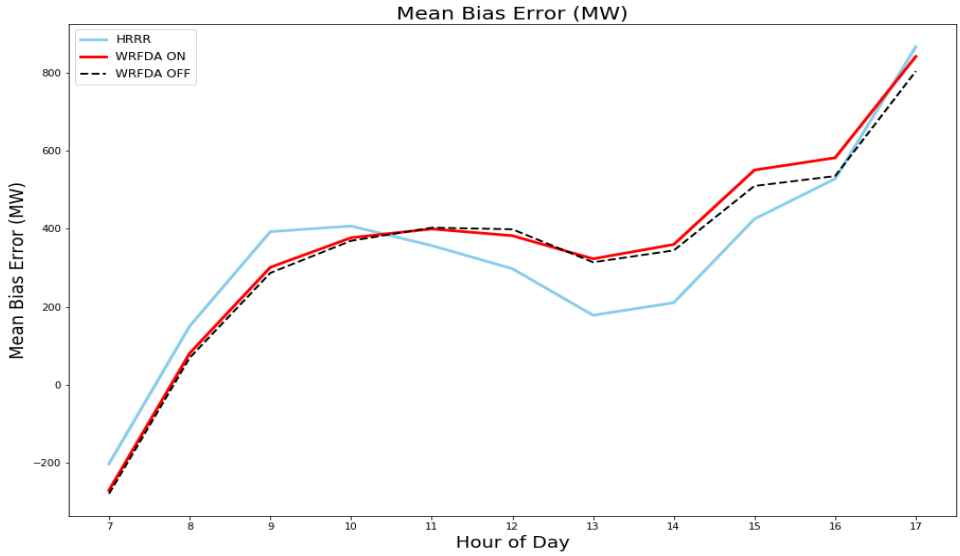

Source: Electric Power Research Institute, 2022.

Root Mean Square Error

The Root Mean Square Error (RMSE) curves for the three methods are shown in Figure 17. In the morning hours, the WRFDA method slightly improves the forecasts, but not in the afternoon hours. The reason is similar to the analysis in the MAE section.

Figure 17: Root Mean Square Error of Solar Forecasts with Different Methods

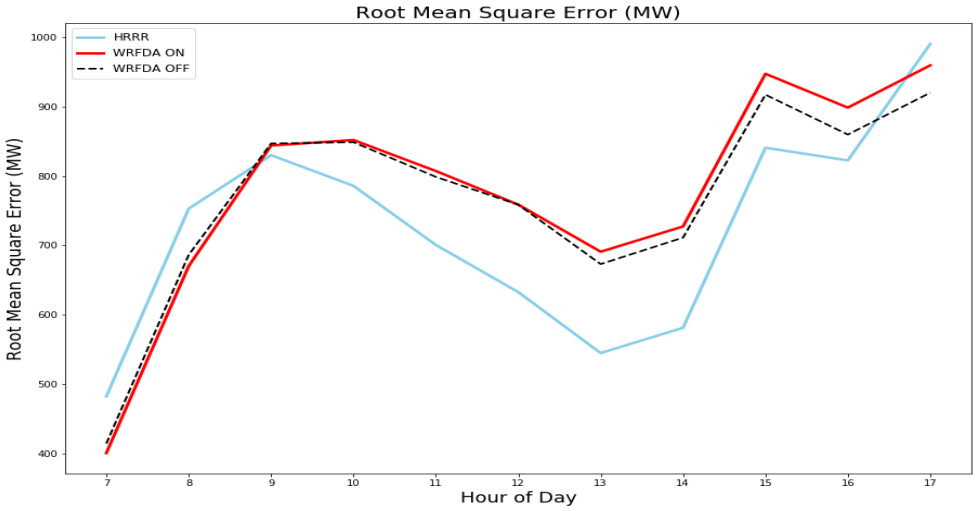

Source: Electric Power Research Institute, 2022.

Normalized Root Mean Squared Error

The Normalized Root Mean Squared Error (NRMSE) curves for HRRR, WRFDA ON, and WRFDA OFF methods are shown in Figure 1814. The normalization factor is the capacity of solar resources in California ISO, which was calculated as 15010 MW in this analysis.

Figure 18: Normalized Root Mean Squared Error of Solar Forecasts with Different Methods

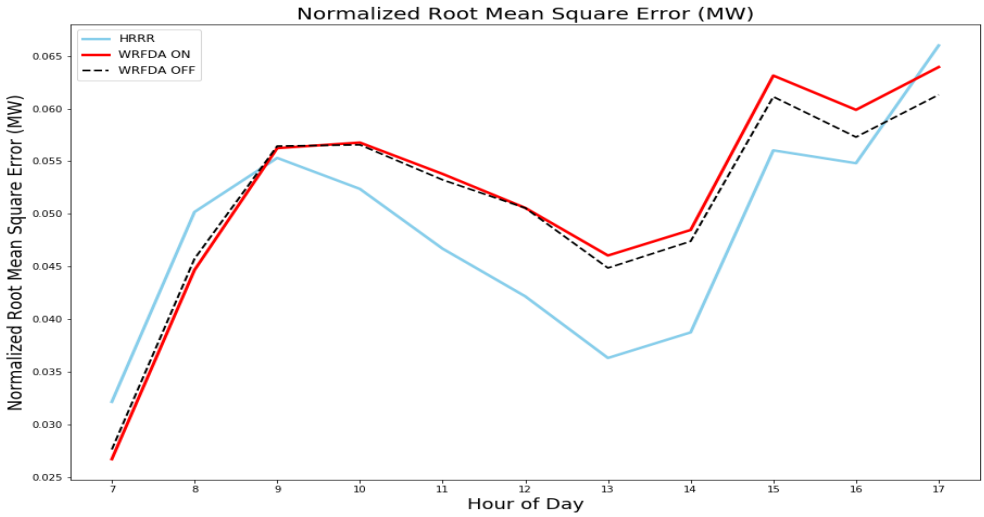

Source: Electric Power Research Institute, 2022.

Forecast Skill Score

By setting the HRRR as the reference forecast, the forecast skill score for WRFDA OFF and WRFDA ON at hours 7, 8, and 17 are shown in Table 15. Positive forecast skill score values mean that the measurement forecast has better performance than the reference forecast. The values in Table 15 range between 0.03 and 0.17, reflecting that the solar forecasting accuracy can be improved by a range between 3 percent and 17 percent with the WRFDA methods.

Table 15: Forecast Skill Score in Selected Hours

Hours	Forecast Score for	Forecast Score for

	WRFDA OFF	WRFDA ON
7	0.14	0.17
8	0.09	0.11
17	0.07	0.03

Source: Sonoma Technology, Inc., 2022

Solar Forecast Value Assessment

This section presents the results of the valuation of solar forecasting through two methods: the historical data analysis method and the production cost simulation method. In the first method, the project team analyzed the California ISO 2018 historical data in terms of solar forecasting, actual solar generation, load payment, solar curtailment, and cleared system reserve quantities. The purpose was to figure out if there exist correlations between solar forecast errors and load payment, curtailment, and reserves in the historical data. In the second method, the project team conducted production cost simulations on two different test systems and quantified the economic and reliability benefits of improved solar power forecasting.

Historical Data Analysis

Description of Available Data

The historical data used for analysis in this section was obtained from the California ISO OASIS and the Oversupply and Curtailments page (California ISO Managing Oversupply). The California ISO OASIS includes data related to the ISO transmission system and its market. The data selected here includes market clearing and locational marginal prices, system demand, solar forecast, and cleared ancillary service. The Oversupply and Curtailments page contains the wind and solar curtailment and generation data in the historical years. In this section, the year 2018 data was used for analysis. The project team analyzed the results for the whole California ISO system instead of individual zones (such as NP15, SP15, and ZP26), although zonal analysis might lead to better conclusions. The reason was because some information needed was only provided on the system level. For instance, the system demand, cleared reserve, and renewable curtailment information was provided for the whole system, not on a zonal basis. Thus, zonal analysis is not included in this report.

Results from Historical Data Analysis

The project team analyzed the correlations of solar forecasting errors and several different evaluation metrics, including load payment, renewable curtailment, and cleared ancillary services. A comprehensive list of results is shown in Appendix E. The results show that there might not exist obvious correlations between the solar forecast errors and the examined metrics. Thus, it is difficult to quantify the value of improved solar forecasting only through analyzing the historical data. Production cost simulation might be needed for this purpose.

Evaluate the Value of Solar Forecasting with Production Cost Simulation Models

Description of Test Systems

The production cost simulation was conducted based on three different test systems: (1) the modified RTS-96 IEEE Reliability test system (NREL, 2018), (2) the WECC 240 Bus Test System (Price, J. et al., 2011), and (3) a modified California ISO system. The IEEE test system was originally developed by NREL with some modifications in this project. The 240-bus WECC test system is a reduced model of the full WECC interconnection. The modified California ISO system was developed based on open-source data from multiple sources. The diagrams of the RTS-96 IEEE Reliability test system and the WECC 240 Bus Test System are shown in Appendix F. The descriptions of the systems are illustrated in what follows.

(1) RTS-96 IEEE Reliability Test System

The one-line diagram of the modified RTS-96 IEEE Reliability test system is shown in Figure F-1 in Appendix F. It has 121 branches, 74 substations, and 278 injectors, of which there are 72 thermal units, one nuclear unit, six wind units, 20 hydro units, 70 PVs, and 109 rooftop PVs. Three load zones are included to mimic the grids for LA Division of Water and Power, Nevada Energy, and Arizona Public Service Company, respectively. The peak load of the system is 8192 MW.

(2) The WECC 240 Bus Test System

The one-line diagram of the WECC 240 Bus Test System is shown in Figure F-2 in Appendix F. The system consists of 240 buses, 139 generators, and 448 branches. System total load is 144 179.1 MW with 206 452.7 MW total generation capacity. Of all the generators, there are 19 coal units, 50 gas units, 29 hydro units, four nuclear units, and 37 renewable units. The 240 buses are located in 22 areas, where the numbers and names of the areas are shown in Table F-1. The connection of the areas is shown in Figure F-3 in Appendix F.

(3) The Modified California ISO Test System

A modified California ISO test system was built with the open-source database. The generation resource data was obtained from the California Public Utilities Commission's public modeling of the integrated resource plan (CPUC 2019-2020). The wind generation, solar generation, and system demand were obtained from the California ISO's Open Access Same-Time Information System (California ISO OASIS). The physical parameters of generation units were obtained from the WECC Transmission Expansion Planning Policy Committee database (WECC TEPPC). Details of the test system are shown below:

- Data obtained from the CPUC 2019-2020: list of generation resources, fuel cost, heat rate and startup cost of thermal generators, maximum/minimum capacity of resources, and hydro generation profile.
- Data obtained from California ISO OASIS: 2019 import energy, reserve requirements (including regulation up, regulation down, spinning, and non-spinning), solar/wind forecast in day-ahead and real-time, and 2019 system demand.
- Data obtained from WECC TEPPC: physical parameters of generation resources.

In addition, the individual solar and wind generation units are not modeled. The total wind and total solar in California ISO are aggregated as a single wind and a single solar unit in the production cost model. Figure F-4 in Appendix F shows the load and solar forecast in day-ahead and real-time in July 2019 in California ISO. The transmission grid network is not modeled. The battery storage capacity in the model is 170 MW.

The project team modeled four operating cycles in the production cost model:

- The week-ahead cycle, which commits units with long start up hours (>12 hours) and high startup costs (> $10k).
- The day-ahead cycle, which runs a unit-commitment model for the next 48 hours. The decision for the first 24 hours is the actual commitment signal that the units must follow. The second 24 hours is the look-ahead horizon, where the decision is used for advisory purpose.
- The hour-ahead cycle, which commits flexible generators with minimum up and down times being less than or equal to one hour.
- The real-time cycle, which dispatches the resources at 5-minute horizon.

(1) Simulation Results for the RTS-96 IEEE Reliability Test System

A summary of the one-month simulation results for the modified RTS-96 IEEE reliability test system is shown in Table 16. The solar penetration level in the base case is about 20 percent. The system operation cost includes two components: the fuel cost of thermal units and the startup cost for calling on related units. Comparing to the base case, the real-time fuel cost and startup cost was reduced by 0.4 percent and 0.5 percent, respectively, in the 20 percent solar improvement case. The area violation occurs when the generation and load balance cannot be met. In PSO, the quantity of the difference between total generation and system demand is the area violation. It is observed that the number of area violation intervals and the quantity of violations in the simulated horizon was reduced by 2.3 percent and 3.3 percent, respectively, in real-time. When the cleared amount of reserve is less than the reserve requirement in the system, a reserve provision violation occurs. The result shows that the quantity of violations for regulation up and spinning down reserves was reduced by 1.1 percent and 1.4 percent, respectively, in real-time.

Table 16: Summary Results of Modified RTS-96 IEEE Reliability Test System

	Base Case	20% Solar Improvement	Changes
Fuel cost ($)	30,857,971	30,734,485	↓ 0.4%
Startup cost ($)	5,716,295	5,687,310	↓ 0.5%
Area violation intervals	969	947	↓ 2.3%
Area violation (MW)	425,820	411,568	↓ 3.3%
Regulation up violation (MW)	94,265	93,181	↓ 1.1%
Spinning down violation (MW)	122,403	120,719	↓ 1.4%

Source: Electric Power Research Institute, 2022.

(2) Simulation Results for the WECC 240 Bus Test System

A summary of the one-month simulation results for the WECC 240 Bus Test System is shown in Table 17. Only DA results are presented, because the RT data was not provided in the original data source. It is observed that when the DA solar forecast had 20 percent improvement, the fuel cost and startup cost in one month were reduced by $902,929 (0.06 percent) and $108,178 (0.4 percent), respectively. This made the total cost savings $1,011,107 in one month. A rough estimation of the annual cost saving would be around $12 million.

Table 17: Summary Results of the WECC 240 Bus Test System for One Month

	Base Case	20% Solar Improvement	Changes

Fuel cost ($)	1,569,386,988	1,568,484,059	↓ 902,929 (0.06%)
Startup cost ($)	5,583,114	5,474,936	↓108,178 (0.4%)

Source: Electric Power Research Institute, 2022.

(3) Simulation Results for the Modified California ISO Test System

The project team run production cost simulations with the modified California ISO test system for July 2019. A summary of the results is shown in Table 18. The total operation cost of the system in July 2019 was about $265.9 million, of which the fuel cost was $260.8 million, and the startup cost was $5.1 million. When 20 percent solar forecast improvement was applied in day-ahead, the fuel cost and startup cost was reduced by $206,000(0.08 percent) and $153,000(3 percent),) respectively. The total cost reduction in July 2019 was $359,000(0.14 percent). A rough estimation of the annual cost saving is $4.3 million. In addition, the improved solar forecast in day-ahead can improve the system's reliability level. As shown in Table 18, the balancing violation was reduced by 2,562 MWh (54 percent) in the month.

Table 18: Summary Results of the Modified California ISO Test System

	Base Case	**20% Solar Improvement**	**Changes**
Fuel cost ($)	260,753,007	260,546,933	↓ 206,074 (0.08%)
Startup cost ($)	5,109,090	4,956,182	↓ 152,908 (3%)
Balancing violation (MWh)	4,750	2,188	↓ 2,562 (54%)

Source: Electric Power Research Institute, 2022.

Grid Impacts Assessment of Improved Solar Forecasting Versus Energy Storage Resource

Base Case Results

The Base Case production cost simulation results for the RTS-96 IEEE Reliability Test System and the Modified California ISO Test System are presented in this section. These results provide an overview of the test systems. The production cost and balancing violation in the Base Case serve as a benchmark for the evaluation of the *Solar Forecast Improvement Case* and *Additional Battery Storage Case*.

(1) RTS-96 IEEE Reliability Test System

Figure 19 shows the hourly generation resource mix profile in one-month in the RTS-96 IEEE Reliability Test System. The total generation by resource types is shown in Table 19. The generation from solar PV and wind accounts for 15.5 percent of the total generation. Other results on the base case are shown in Appendix F.

Figure 19: Resource Generation Mix in the RTS-96 IEEE Reliability Test System

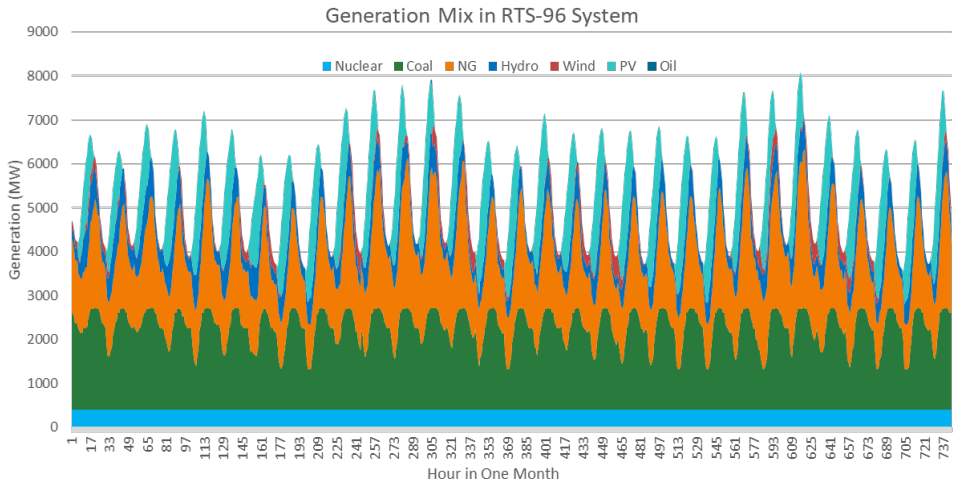

Source: Electric Power Research Institute, 2022.

Table 19: Total Generation by Resource Types in RTS-96 IEEE Reliability Test System in One Month

Resource Type	Total Generation (MWh)	Percentage (%)
Nuclear	297,600	7.5
Coal	1,405,151	35.3
NG	1,275,271	32.1
Hydro	380,247	9.6
Wind	77,335	1.9
PV	538,904	13.6
Oil	788	0

Source: Electric Power Research Institute, 2022.

(2) The Modified California ISO Test System

The generation mix of resources for the peak load day (July 24, 2019) is shown in Figure 20. The total generation by resource type in July is shown in Table 20. The percentages of the resources in different types are very close to those published in the California ISO market performance report (California ISO, 2019).

Figure 20: Resource Generation Mix in the Modified CAISO Test System in Peak Day

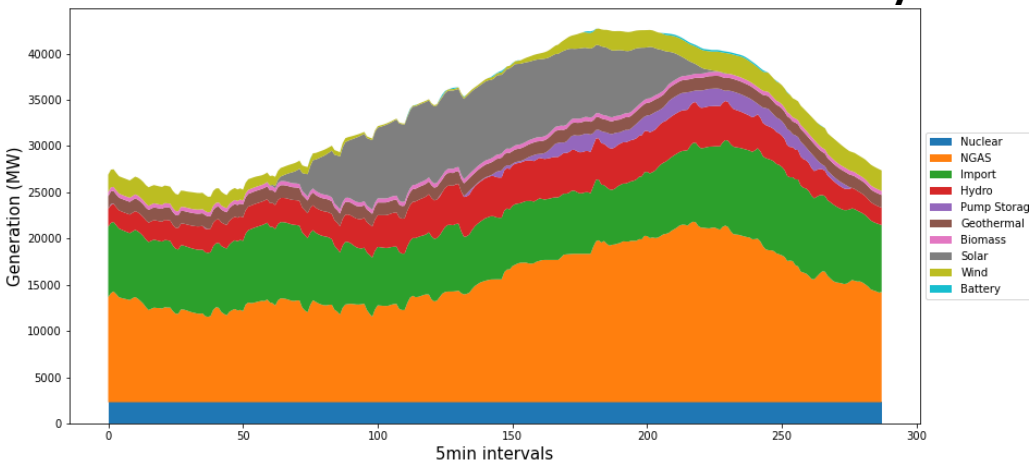

Source: Electric Power Research Institute, 2022.

Table 20: Total Generation by Resource Types in the Modified California ISO Test System in One Month

Resource Type	Total Generation (MWh)	Percentage (%)
Nuclear	20,534,400	8.1
NGAS	69,798,207	27.7
Hydro	31,181,524	12.4
Pumped Storage	2,862,015	1.1
Import	54,105,940	21.5
Geothermal	12,229,592	4.8
Biomass	3,936,289	1.6
Solar	38,066,222	15.1
Wind	19,307,350	7.7
Battery	209,038	0.1

Source: Electric Power Research Institute, 2022.

Quantifying the Benefits of Battery Storage Versus Improved Solar Power Forecast

RTS-96 IEEE Reliability Test System

Improving 20 percent solar forecasting performance in the day-ahead, the system operating cost and balancing violation was reduced by 0.4 percent and 3.3 percent, respectively. To compare the system's benefits of improved solar forecasting and energy storage, the project team conducted sensitivity studies by adding 50 MW, 70 MW, and 100 MW to 4-hour battery storage systems. Cost reduction relative to the Base Case is shown in Figure 21; balance violation reduction relative to the Base Case is shown in Figure 22. In adding 70 MW of battery storage, the system's operating cost was reduced by 0.39 percent and the balancing violation was reduced by 1.52 percent. This was a similar cost benefits as 20 percent solar forecasting improvement in day-ahead; however, the balancing violation reduction was smaller—1.52 percent compared to 3.3 percent from solar forecasting improvement.

Figure 21: Percentage of Cost Reduction Relative to the Base Case

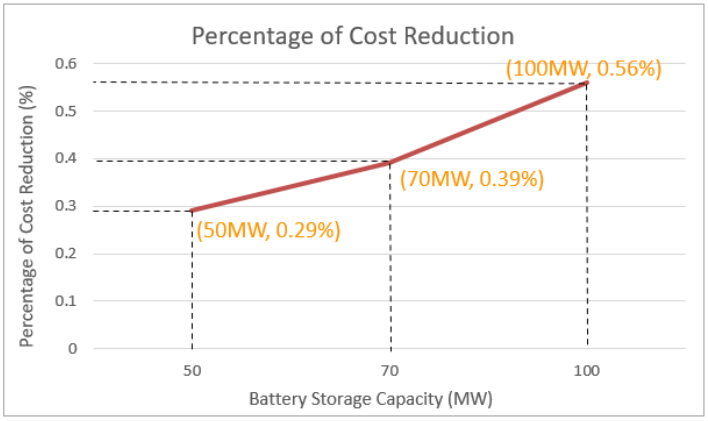

Source: Electric Power Research Institute, 2022.

Figure 22: Percentage of Balancing Violation Reduction Relative to the Base Case

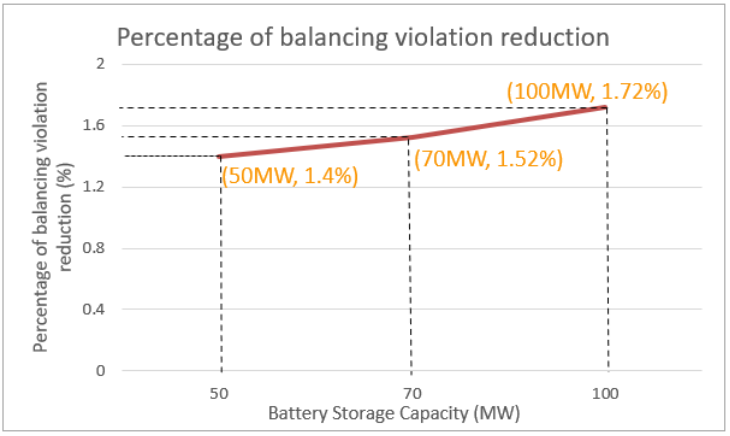

Source: Electric Power Research Institute, 2022.

The Modified California ISO Test System

In this section, different battery storage capacities were added to the Base Case and production cost simulations were conducted. A summary of the simulation results for various cases is shown in Table 21. 25 MW, 50 MW, and 100 MW battery storage capacity was added to the Base Case separately. The evaluation metrics included fuel cost, startup cost, balancing violation, and solar curtailment. The following observations were made from Table 21:

- The marginal benefit of adding battery storage is decreased. For instance, when the battery capacity is increased from 25 MW to 50 MW, the fuel cost reduction is increased from $253,480 to $556,477. However, when the battery capacity is further increased to 100 MW, the fuel cost reduction is only $562,372.
- The solar forecast improvement has greater impact on the startup cost than battery storage. The 20 percent solar forecast improvement leads to $152,908 startup cost reduction; adding 100 MW battery storage only leads to half of this number. Solar forecast improvement reduces the uncertainty of the grid operation, such that the system would rely less on calling up expensive gas units to meet the system demand in real-time. Adding battery storage can increase the system's operational flexibility but cannot reduce the uncertainty.

- Similarly, the solar forecast improvement has greater impact on the balancing violation than battery storage. The balancing violation in real-time occurs because the unit commitment decisions are made in the previous cycles (for example, day-ahead), and the system lacks sufficient flexibility to commit and decommit units to meet the delta net demand (specifically, the difference of forecasted net demand between day-ahead and real-time) in real-time. The solar forecasting improvement can decrease the "delta net demand", and thus reduce the balancing violation.
- The solar curtailment quantity keeps decreasing when more battery capacity is added to the system.

Table 21: Results Summary for Various Cases

Cases	Fuel cost ($)	Startup cost ($)	Balancing Violation (MWh)	Solar Curtailment (MWh)
Base Case	260,753,007	5,109,090	4,750	15,750
20% Solar Forecast Improvement	260,546,933 (↓206,074)	4,956,182 (↓152,908)	2,188 (↓2,562)	13,465 (↓2,285)
Adding 25 MW Battery	260,499,527 (↓253,480)	5,063,624 (↓45,466)	4,629 (↓121)	12,984 (↓2,766)
Adding 50 MW Battery	260,196,530 (↓556,477)	5,058,418 (↓50,672)	4,433 (↓317)	11,751 (↓3,999)
Adding 100 MW Battery	260,190,635 (↓562,372)	5,031,617 (↓77,473)	4,391 (↓359)	10,662 (↓5,088)

Source: Electric Power Research Institute, 2022.

Figure 23 shows the percentages of production cost reduction relative to the Base Case, where the production cost is the sum of fuel cost and startup cost. The 20 percent solar forecasting improvement reduces the production cost by 0.14 percent and a 25 MW battery reduces the production cost by 0.11 percent. The economic benefit of 20 percent solar forecasting improvement, if only measured by the production cost, is close to that of 25 MW battery storage capacity in the system.

Figure 23: Percentage of Production Cost Reduction Relative to the Base Case

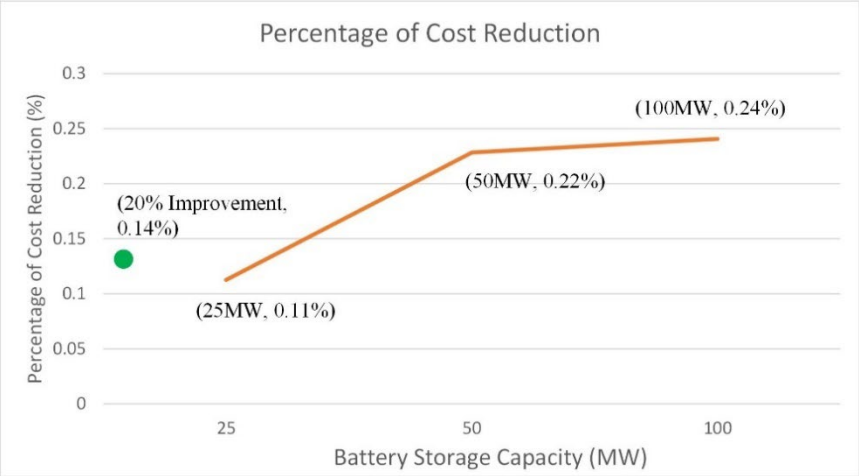

Source: Electric Power Research Institute, 2022.

Figure 24 shows the percentages of balancing violation reduction relative to the Base Case. The green dot shows the percentage of 20 percent solar forecasting improvement. As statedthe solar forecasting improvement has more significant impact on balancing violation than adding battery storage capacity.

Figure 24: Percentage of Balancing Violation Reduction Relative to the Base Case

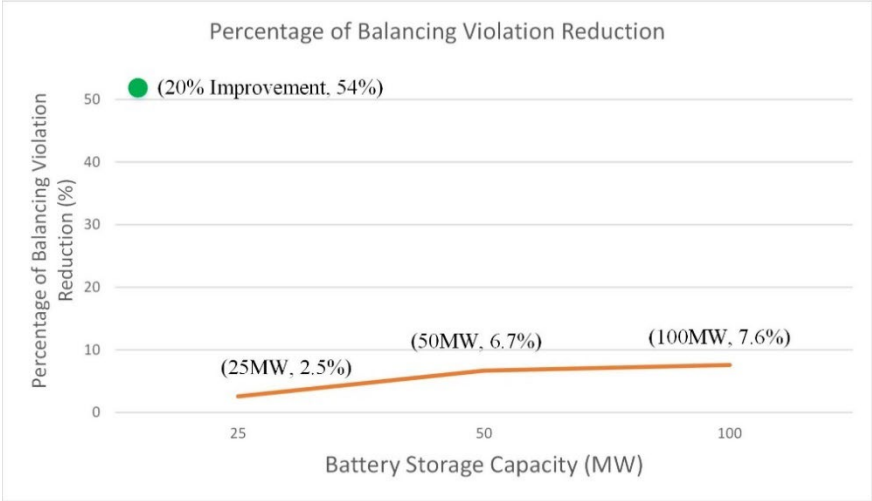

Source: Electric Power Research Institute, 2022.

Figure 25 shows the percentages of solar curtailment reduction relative to the Base Case. A 20 percent solar forecasting improvement reduces the curtailment by 14.5 percent, which is closest to the effect of 25 MW added battery storage capacity.

Figure 25: Percentage of Solar Curtailment Reduction Relative to the Base Case

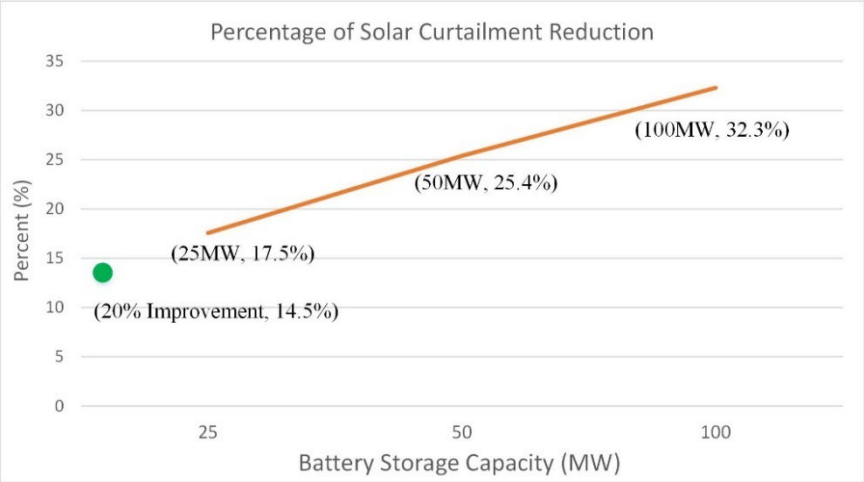

Source: Electric Power Research Institute, 2022.

CHAPTER 4: Technology/Knowledge/Market Transfer Activities

This chapter summarizes the technology and knowledge transfer activities to disseminate research findings, solicit feedback from industry leaders, and improve results and recommendations.

Technology Transfer Activities

This project relied on robust multi-disciplinary collaboration between technical experts in data science, meteorological measurement and forecasting, and grid operations to achieve core research objectives. The TAC included engaged members from California ISO, Clean Power Research, NOAA, Pacific Gas and Electric Company, and Southern California Edison. Four TAC meetings were held at various stages of the project to share results, methods, and preliminary results from each project task. The project team delivered information through presentations, interim project reports, and post-meeting reports that included question and answer responses. These meetings provided vital feedback to the research team that guided future activities. In addition to TAC meetings, a real-time data website was set up and maintained throughout the project to visualize data collected from all meteorological instruments during the field campaign. During the project timeframe, this website was available to research team members and project stakeholders, though it is longer active since the completion of the project. Input from the California ISO and other stakeholders was also solicited throughout the project with regard to solar forecast value assessment and integration into grid operations. This report along with final meeting materials and fact sheets will also be made publicly available by the CEC.

The project team presented the major outcomes of this project at the following conferences:

- "Improving Coastal and Valley Fog Forecasts by Assimilating Boundary Layer Observations", 100th American Meteorological Society Annual Meeting, Jan. 2020.
- "Predicting Fog and Stratus Dissipation for Solar Energy Applications in California Using Meteorological Measurements and Machine Learning", 12th Conference on Weather, Climate, and the New Energy Economy, January 12-16, 2021.

Real-Time Data Website Development for Project Stakeholders

The project team developed a real-time data website to support the field program (Craig et al., 2018). The website was a key endpoint of the real-time data acquisition system and provided an interface for visualizing, reviewing, and quality-assuring sensor data. The website also served as a portal for visualizing the sensor data that were being collected. The web address was https://cecsolar.sonomatechdata.com, and the research team provided authentications to project stakeholders upon request.

The website focused on the specialized sensor data being collected for this project. The specialized sensor data augmented existing meteorological observations, such as data from the NWS surface and upper-air observation networks, as well as satellite data from the National Aeronautics and Space Administration (NASA), which were used to improve numerical

weather prediction forecasts and develop short-term (15 minute to 1 hour) statistical forecasts of fog formation and dissipation.

The project team used cellular communications and file transfer protocol (FTP) to:

- Ensure reliable communications with each site.
- Ensure high data recovery rates for real-time data use.
- Monitor instrument performance.
- Remotely diagnose instrument problems.
- Make instrument system changes as needed.

Each site was equipped with dual-band cellular modems that automatically pushed data every 30 minutes (60 minutes for the RWP/RASS) from each site to FTP servers. Once the data were uploaded, automatic processes took the data in their raw form and stored them in a Microsoft® SQL Server® database, effectively combining all data into a single data set. Raw data files were stored and backed up each day. Other automated processes generated images of the data and uploaded them to the project website. The real-time data website (described in the following section) facilitated the quality assurance and troubleshooting process, allowing the research team to quickly identify and address data flow and instrument issues throughout the field measurement campaign. The data were provided every 30 minutes (60 minutes for the RWP/RASS) to a secured Amazon S3 cloud storage solution to facilitate data dissemination to project partners and stakeholders. Meteorological observations were also delivered to the Meteorological Assimilation Data Ingest System, unless prohibited by third-party data owners.

Development and Transfer of Measurements Using Sensors Technology

Development: The project team successfully completed a measurement program involving targeted deployment of ground-based atmospheric boundary layer sensors from December 2017 through March 2019 to support improvements in predicting fog and stratus dissipation in high solar penetration regions of California. Unique data were collected throughout California for several dozen marine stratus days and about one dozen radiation fog days. The measurement program involved augmenting existing sensor networks with new sensor deployments. The instrument network consisted of five RWPs, seven sodars, six ceilometers, and two radiometers spread across the ten core and supplemental measurement sites. These boundary profile measurements augmented the wealth of meteorological data available from routine observation networks. Data were collected with high reliability and completeness for most instruments and sites throughout the data collection period.

Transfer: A key success of the measurement program was the successful integration of new sensor deployments within ng existing sensor networks. The nine pre-existing site locations used for this project were owned and operated by air quality management districts to serve local and regional air quality forecasting and management needs. Significant coordination between the project team and data providers was needed to arrange site access and data sharing logistics, and this coordination allowed for unique data to be collected at a substantial cost savings compared to acquiring, siting, and operating new instruments. The technology developed in this project will be used to coordinate similar efforts in the future for California users by Sonoma Technology, Inc. Given that much of the instrumentation leveraged in this project is still operational, there may be opportunities for future collaborations that can

provide important boundary layer profile measurement data for weather, air quality, and energy applications that directly benefit the public.

Another technology transfer activity was conducted through a collaboration with NEXTracker, a company that develops solar tracker systems and solar energy solutions. The project team and NEXTracker successfully deployed new sensors at the Fremont core site, which was located at the edge of the San Francisco Bay and was well suited to collect measurements of marine stratus.

End Users and Benefits

The project team discussed the improved WRF-Solar forecasts identified during this project with targeted end users. The primary end users were stakeholders involved with the daily operations of California's electric power system, including:

- California ISO.
- Public and private electricity distribution utilities (for example, Southern California Edison [SCE], Pacific Gas and Electric [PG&E], San Diego Gas and Electric [SDG&E], Sacramento Municipal Utility District [SMUD]).
- Owners/operators of commercial-scale solar generation facilities.
- Participants in the California energy markets (such as traders associated with financial institutions, owners of non-solar generation facilities, etc.).
- Owners of residential or industrial buildings with rooftop solar and energy storage systems (ESS) who may use forecasts to optimize the use of these technologies to manage energy costs.

The project team organized regular meetings with California ISO experts in 2019 to discuss the proposed methodology to quantify the value of improved solar power forecasting. Key personnel in the project team made a site visit to SCE in 2019 to discuss how to implement the improved solar forecasting method and data. End users from other companies like PG&E have followed this project through TAC meetings.

Improved short-term renewable forecasts would provide benefits to California ISO operations, benefitting all California ratepayers, as well as improve individual IOU transmission, distribution, and procurement decisions. From the perspective of the California ISO, improved forecasts of marine layer and fog conditions have the potential to improve the efficiency of generation dispatch, reduce the need for operating reserves to manage forecast error, and maintain or increase reliability while integrating increased levels of renewables. There are numerous potential benefits for California's electric utilities. For example, several PG&E business applications require accurate solar forecast data for both utility-scale and customer-side, distributed generation (DG) solar purposes. These include load forecasting and utility-scale and DG forecasting for energy procurement purposes, as well as transformer-thermal-limit and line-voltage-variability-violation predictions for electric distribution operations.

One deficiency noted by the PG&E meteorology group in the presently available NWP models is the ability to accurately predict the progression and dissipation of summertime marine stratus along the California coast and through the San Francisco Bay Area, as well as radiation fog burn-off timing for the San Joaquin Valley. Improving the forecasting methods around these weather phenomena will help to better assess utility-scale and distributed solar PV output and variability and their direct and derivative effects on market participation and

distribution grid operations. Specifically, providing accurate short-term (0 to 6 hour) and day-ahead forecasts of solar irradiance will allow for more efficient, effective, and reliable grid operations. The importance of improving solar forecast accuracy will only increase over the coming years as additional solar capacity will be brought into service to meet California's aggressive RPS goals.

Two methods for quantifying the value of solar power forecasting were adopted in this report: the historical data analysis method and the PCM simulation method. Results from historical data analysis show that there may not exist a simple correlation between the solar forecast error and the interested evaluation metrics. Thus, it is difficult to quantify the value of solar forecasting from studying and analyzing the historical data only. The PCM simulation results show that with 20 percent solar forecast accuracy improvement in day-ahead, the fuel cost and startup cost of thermal units in the system can be reduced by between 0.06 percent and 1.2 percent, depending on test systems and market cycles. In addition, the violations on area balancing and reserves were seen reduced with improved solar forecast accuracy.

CHAPTER 5:
Conclusions and Recommendations

Conclusions are summarized in this section by major project tasks. For each task, the key findings and recommendations based on the work are provided.

Field Data Collection

Key Findings

A measurement program involving targeted deployment of ground-based atmospheric boundary layer sensors was successfully completed from December 2017 through March 2019 to support improvements in predicting fog and stratus dissipation in high solar penetration regions of California. Unique data were collected throughout California for several dozen marine stratus days and about one dozen radiation fog days. The measurement program involved augmenting existing sensor networks with new sensor deployments. The instrument network consisted of five RWPs, seven sodars, six ceilometers, and two radiometers spread across ten core and supplemental measurement sites. These boundary profile measurements augmented the wealth of meteorological data available from routine observation networks. Data were collected with high reliability and completeness for most instruments and sites throughout the data collection period.

Recommendations

A key success of the measurement program was the successful integration of existing sensor networks with new sensor deployments. Significant coordination between the project team and data providers was needed (and achieved) to arrange site access and data sharing logistics, and this coordination allowed for unique data to be collected at a substantial cost savings compared to acquiring, siting, and operating new instruments. This successful measurement program can serve as a model for coordinating similar efforts in the future. Key challenges from this measurement program were suitably locating sodar and RASS instrumentation (because of the audible noise they emit), untimely breakdowns of the microwave radiometer, and the limited number of winter radiation fog days that occurred in the San Joaquin Valley during the measurement period.

Instruments used for a research project are often decommissioned after the research project has concluded. By design, this research project leveraged existing operational instruments whenever possible. Nine of the ten measurement sites used in this project were owned and operated by air quality management districts to serve local and regional air quality forecasting and management needs, and many of the instruments at those sites remain operational. Research consistently shows that data from boundary layer sensors, particularly wind profilers, can improve weather, air quality, and energy forecasts, especially when the sensors fill substantial data gaps in existing operational measurement networks. Given the overlapping benefits, there may be opportunities to pursue partnerships with utilities, air quality management districts, NOAA, universities, and the private sector to maintain and expand operational wind profiler instrument networks in California.

Physics Based & Statistical Modeling

Key Findings

Forecasts of solar electric generation in California depend heavily on accurate forecasts of fog and boundary layer cloud formation and persistence. The experiments showed that the WRF model's fog forecasts were strongly modulated by the choice of boundary layer scheme and by parameter value choice in the modified version of the YSU scheme that was tested. The impact of these parameterization choices themselves depended heavily on the initial conditions on each forecast day.

Assimilation of local observations of boundary layer temperature, humidity, and wind using the WRF three-dimensional variational data assimilation scheme showed a small positive impact on the near-term forecast quality.

Recommendations

Probabilistic forecasts of solar electric generation in California may be improved by the use of a perturbed-physics ensemble system tailored specifically for local forecast error sources relating specifically to valley and coastal fog persistence. The physics variations in this ensemble would be focused cloud-topped boundary layer entrainment. Several WRF runs were made for each forecast, with differing values of the parameter governing cloud-topped boundary layer entrainment. This ensemble would be expected to exhibit differing levels of forecast spread, depending on the initial conditions, and this ensemble spread would be expected to correspond to forecast uncertainty. A few years of historical ensemble experiments would be required to diagnose this spread-error relationship.

Machine Learning for Very Short-Term Predictions

Key Findings

Machine learning models for predicting cloudiness and solar irradiance at 15-minute to 2-hour forecast horizons based on time series data from the field campaign were tested and evaluated. The machine learning models yielded reasonable results at predicting cloudiness and solar irradiance (forecast accuracy greater than 95 percent for cloud predictions, and a RMSE between 65 and 70 W/m^2 for solar irradiance predictions). The machine learning models outperformed a persistence baseline forecast beyond the 15-minute forecast horizon but were no better than a persistence forecast at the 15-minute forecast horizon.

Adding the project sensor data to the machine learning models resulted in 4-23 percent improvement in cloud predictions compared to baseline machine learning models that only used synoptic meteorological data. Forecast performance was not as good when the machine learning models were extended to also include prediction of cloud transitions (as opposed to just prediction of cloudy or cloud-free conditions), leaving significant room for improvement. Ceilometer cloud base, solar irradiance, and wind profiler data below 1 km were identified as important predictors in the machine learning models. Model performance was not always best when using all available project sensor data, but models that included wind profiler data generally outperformed models that excluded wind profiler data. The benefit of including radiometer data in the machine learning analysis was inconclusive, as forecast performance for

scenarios that included radiometer data was not always better than for scenarios that excluded radiometer data.

Recommendations

Future follow-up analysis work that could be considered to further improve the ML-based models of cloudiness and solar irradiance include:

- Use the "early stop" feature in XGBoost to improve the performance for the transitions between cloudy and clear sky conditions.
- Use "up-sampling" to further address the issue of unbalanced classifications that arises because cloud transitions are much less frequent in the data compared to the "stratus" or "clear sky" data classifications.
- Apply hyperparameter tuning for predicting surface solar irradiance.
- With sufficient sample size, develop ML models of cloud cover and solar irradiance using deep learning techniques such as neural networks.
- Separate specific radiometer parameters (such as temperature, water vapor mixing ratio, and integrated vapor and liquid water) in the sensitivity analysis to help isolate the specific radiometer data that may provide the most benefit to the ML forecasts, and to help further characterize the role and importance of radiometer data in the ML predictions.
- Collect additional wintertime field measurement data in the Central Valley to facilitate a robust ML-based analysis of fog development and burn-off in this area.
- Extend the ML model development work and incorporate satellite data to develop a general application beyond the sites that have targeted data available.

Solar Forecasting Value Assessment

Historical Data Analysis

Key Findings

The project team analyzed the California ISO 2018 historical data in terms of LMPs, demand, solar forecast, solar generation, solar curtailment, and awarded ancillary services. Various correlation analyses were conducted including:

- Correlation analysis between actual solar forecasting error and interested metrics (such as load payment, solar curtailment, and awarded quantity of reserves) on interval basis.
- Correlation analysis between daily MAE or RMSE of solar forecasting and interested metrics (such as load payment, solar curtailment, and awarded quantity of reserves).
- Monthly analysis by grouping the historical data by month of year.
- Hourly analysis where the historical data was grouped by hour of day.

However, statistics results showed that there might not exist a strong correlation between solar forecast error and the interested metrics. For example, a high load payment might occur when the RMSE of solar forecasting was either large or small. This occurred in both DA and RT forecasts, and in both annual and monthly analysis. The reason might be because the system operation condition was very complicated, and there might not exist a simple relationship between forecast errors and interested metrics such as load payment, solar curtailment, and awarded quantity of reserves.

Recommendations

Quantifying the value of solar power forecasting accuracy only through historical data analysis might not be desirable. The solar forecasting error is random, and the system operation condition is complicated. There might not exist a simple correlation between the two. Note that all of the analyses were based on the whole California ISO system, not on individual resources. It might be more meaningful to analyze the historical data on individual resources, because the number of factors to impact a single resource is much less.

Production Cost Modeling Analysis

Key Findings

The research team conducted PCM analysis on the modified RTS-96 IEEE Reliability test system, the WECC 240 Bus Test System, and the modified California ISO test system. Day-ahead solar forecasting accuracy was uniformly improved by 20 percent in all intervals. Test results on the IEEE system show that the real-time fuel cost and startup cost was reduced by 0.4 percent and 0.5 percent, respectively, for 20 percent solar forecasting accuracy improvement. In addition, the number of balancing violation intervals and the quantity of the violations in RT was reduced by 2.3 percent and 3.3 percent, respectively, and the quantity of violations for regulation up and spinning down reserves was reduced by 1.1 percent and 1.4 percent, respectively, in RT. Test results on the WECC-240 Bus Test System show that the fuel cost and startup cost was reduced by 0.06 percent and 0.4 percent, respectively. Finally, test results on the modified California ISO test system shows that the fuel cost, startup cost, and balancing violation was reduced by 0.08 percent, 3 percent, and 54 percent, respectively.

Recommendations

Although a California ISO-like test system was built with the open-sourced database, it is still worth conducting future tests with actual California ISO resources and network data. One could build the production cost model with the actual data to mimic the operation of the California ISO system and utilize the improved solar forecasting accuracy data on individual resources. One could also test the benefits of improved solar forecasting accuracy under different solar penetration scenarios.

Grid Impacts Assessment of Improved Solar Forecasting Versus Energy Storage Resource

Key Findings

The project team compared the economy and reliability benefits of improved solar forecasting to energy storage resources. In the modified California ISO test system, a 20 percent solar forecasting improvement in day-ahead can reduce the total system operating cost by 0.14 percent. This is similar to the effect of a 25 MW battery storage resource which reduces the operating cost by 0.11 percent. However, the solar forecasting improvement leads to much higher reductions on the startup cost of thermal units because it reduces the grid operation uncertainty between day-ahead and real-time.

Recommendations

It was shown in Lazard (2019) that the Levelized Cost of Energy (LCOE) for a 100 MW, 4-hour energy storage system is between $165 and $305 per MWh. If linearly interpolated, the LCOE

for a 25 MW, 4-hour battery resource is between $41.25 and $76.25 per MWh. In the modified California ISO test system, the total generation of the 25 MW battery storage system in one month is about 3,000 MWh. This leads to the monthly average net present cost being between $124,000 and $229,000. Note that these values are rough estimations. More accurate analysis should be conducted in the future. In addition, it would be helpful to estimate the cost of solar forecasting improvements for better comparisons.

CHAPTER 6:
Benefits to California Ratepayers

Quantitatively stating the benefits of improved solar forecasting can be difficult given the numerous interactions among potential benefits. Moreover, the accrual of benefits is also based on how forecasts are used, the generation mix that is exposed to improved forecasts, and other economic factors such as natural gas prices, carbon prices, and value of lost load. This project used production cost modeling (PCM) simulations on representative test systems with and without improved solar forecasts. While the results of these exercises were not obtained by testing the actual California power system, they provided robust estimates of the benefits attributable to improved solar forecasts.

This project also analyzed the actual historical data from California ISO, with the purpose of identifying and understanding relationships between forecast error and several California ISO variables of interest. However, test results showed that there might not exist a simple relationship between solar forecast errors and metrics of interest (such as load payment, renewable curtailment, and cleared reserves quantity) for the whole California ISO system, due to the dimension of complexity in system operations.

To overcome this difficulty, it is suggested to analyze the historical data on individual solar plants, because the factors that impact a single plant are much less. On the other hand, the PCM studies used three test systems: the modified RTS-96 IEEE reliability test system; a reduced-form WECC system with 240 buses; and a modified California ISO test system. Test results on the modified RTS-96 system show that the monthly fuel cost and startup cost was reduced by 0.4 percent ($123,486) and 0.5 percent ($28,985), respectively, when the solar generation forecast was improved by 20 percent compared to historical data. In addition, the real-time area balancing violation in a month reduced from 425,820 MWh to 411,568 MWh, a reduction of 3.3 percent. Test results from the reduced WECC system show that the fuel cost in one month were reduced by $902,929 (a reduction of 0.06 percent), and unit start-up cost in one month were reduced by $108,178 (0.4 percent) for 20 percent solar power forecast improvements. The total cost saving in the examined month was approximately $1.01 million, which leads to an annual total cost saving of $12.12 million. Test results on the modified California ISO system show that fuel cost and startup cost in July 2019 was reduced by $206,074 (0.08%) and $152,908 (3%), respectively, for 20 percent solar power forecast improvements in day-ahead. The total production cost reduction in the month was $359,000 (0.14%). A rough estimation of the annual cost saving was $4.3 million. These savings translate into energy procurement cost savings for IOUs and lower electricity rates for end-use customers.

As the number of installed solar systems continues to increase over time, the benefits of improved forecasting that lead to more efficient bulk power system operations will become more pronounced. The project team also compared the grid impacts of solar forecasting improvement and energy storage resources. Simulation results from the modified California ISO test system show that the economic benefit of 20 percent solar forecasting improvement in day-ahead is close to that of adding 25 MW of battery storage to the system, but the former can bring significantly higher reliability to the grid than the latter. The reliability benefit was measured by the percentage of balancing violation reductions, whose value was 54 percent for

solar forecasting improvement and only 2.5 percent for adding 25 MW of battery storage. Considering the investment cost and environmental impacts of building a battery storage resource, the solar forecasting improvement approach is (likely) less expensive and has almost no environmental concerns. This will bring additional benefits the California ratepayers.

GLOSSARY AND LIST OF ACROYMNS

DA: day-ahead

DG: distributed generation

EPRI: Electric Power Research Institute

FTP: file transfer protocol

GHI: Global Horizontal Irradiance

GOES: Geostationary Operational Environmental Satellite

HRRR: High Resolution Rapid Refresh

IOU: investor-owned utilities

ISO: Independent System Operator

LAX: Los Angeles International Airport

LCOE: Levelized Cost of Energy

MAE: Mean Absolute Error

MAPE: Mean Absolute Percentage Error

ML: machine learning

NASA: National Aeronautics and Space Administration

NCAR: National Center for Atmospheric Research

NEXTracker: NEXTracker, Inc.

NOAA: National Oceanographic and Atmospheric Administration

NREL: National Renewable Energy Laboratory

NWP: Numerical Weather Prediction

PCM: production cost modeling

PG&E: Pacific Gas and Electric

PSO: Power System Optimizer

PV: solar photovoltaics

RASS: radio acoustic sounding system

RF: Random Forest

RMSE: Root Mean Square Error

RPS: Renewable Portfolio Standards

RRTMG: Rapid Radiative Transfer Model used in the Global Forecast System

RT: real-time

RTS: Reliability Test System

RWP: radar wind profilers

RWP: radar wind profilers

SCE: Southern California Edison

SDG&E: San Diego Gas and Electric

SHAP: SHapley Additive exPlanations

SJVAPCD: the San Joaquin Air Pollution Control District

SMAQMD: the Sacramento Metropolitan Air Quality Management District

SMUD: Sacramento Municipal Utility District

STI: Sonoma Technology, Inc.

TAC: technical advisory committee

UC: unit commitment

WECC: Western Electricity Coordinating Council

WRF: Weather Research and Forecasting

WRFDA: The Weather Research and Forecasting model data assimilation

XGBoost: extreme Gradient Boosting

YSU: Yonsei University

REFERENCES

Alessandrini, A., Della Monache, S.L., Sperati, S., Cervone, G. 2015. An analog ensemble for short-term probabilistic solar power forecast. Applied Energy, 157:95-100, doi: 10.1016/j.apenergy.2015.08.011.

Baldocchi, D., Waller, E. 2014. Winter fog is decreasing in the fruit growing region of the Central Valley of California, Geophys. Res. Lett., 41, 3251–3256, doi:10.1002/2014GL060018.

Barker, D.M., et al., 2012. The Weather Research and Forecasting Model's Community Variational/Ensemble Data Assimilation System: WRFDA. Bull. Amer. Meteor. Soc., 93, 831–843.

Bartokova I., Bott A., Bartok J., and Gera M. 2015. Fog prediction for road traffic safety in a coastal desert region: improvement of nowcasting skills by the machine-learning approach. Boundary Layer Meteorology, 157, 501-516, 2015

Benjamin, S. G., and Coauthors. 2016. A North American hourly assimilation and model forecast cycle: The Rapid Refresh. Mon. Wea. Rev., 144, 1669–1694, https://doi.org/10.1175/MWR-D-15-0242.1.

Benjamin, S., et al. 2016. A North American Hourly Assimilation and Model Forecast Cycle: The Rapid Refresh. Monthly Weather Review. https://doi.org/10.1175/MWR-D-15-0242.1

Bianco, L., et al., 2019. Impact of model improvements on 80 m wind speeds during the second Wind Forecast Improvement Project (WFIP2), Geosci. Model Dev., 12, 4803–4821, https://doi.org/10.5194/gmd-12-4803-2019, 2019.

Breiman L. 2001. Random Forests. Machine Learning, 45, 5-21, https://doi.org/10.1023/A:1010933404324.

Bretherton CS, McCaa JR, Grenier H. 2004. A new parameterization for shallow cumulus convection and its application to marine subtropical cloud-topped boundary layers. I. Description and 1D results. Mon Weather Rev 132:864–882.

California ISO (2018). BPM for market operations, version 58. Revised: November 29, 2018.

California ISO OASIS. http://oasis.caiso.com/mrioasis/logon.do.

California ISO Managing Oversupply. www.caiso.com/informed/Pages/ManagingOversupply.aspx

California ISO Market (2019), http://www.caiso.com/market/Pages/MarketProcesses.aspx

CAISO (2019). 2019 Annual report on market issues and performance. June 2020.

CAISO (2020). Largest battery storage system in US connects to California ISO grid. July 13, 2020.

Chen, T., and Guestrin C. 2016. XGBoost: A Scalable Tree Boosting System. KDD '16: Proceedings of the 22nd ACM SIGKDD International Conference on Knowledge Discovery and Data Mining. Pages 785-794. ISBN: 978-1-4503-4232-2.

Chow C.W., Urquhart B., Lave M., Dominguez A., Kleissl J., Shields J., and Washom B. 2011. Intra-hour forecasting with a total sky imager at the UC San Diego solar energy testbed. Solar Energy, 85(11), 2881-2893, doi: 10.1016/j.solener.2011.08.025.

Cooperman A., van Dam C.P., Zack J., Chen S.-H., and MacDonald C. 2018. Improving short-term wind power forecasting through measurements and modeling of the Tehachapi Wind Resource Area. Final project report by the California Wind Energy Collaborative, Davis, CA, CEC-500-2018-002, February. https://www.energy.ca.gov/2018publications/CEC-500-2018-002/CEC-500-2018-002.pdf.

CPUC (2019-2020). IRP Events and Materials. https://www.cpuc.ca.gov/General.aspx?id=6442459770.

Craig K.J., Moffet R.C., and MacDonald C.P. 2018. Measurements of fog burn-off for improved solar forecasting: real-time data website report. Prepared for the Electric Power Research Institute, Palo Alto, CA, by Sonoma Technology, Inc., Petaluma, CA, STI-917071-6879, March 1.

Edelson, D. 2017. Large Scale Solar Integration. Presentation in the Market Issues Working Group (MIWG) meeting, September 25, 2017, Rensselaer, NY.

Ela, E., Diakov, V., Ibanez, E., Heaney, M.. 2013. Impacts of Variability and Uncertainty in Solar Photovoltaic Generation at Multiple Timescales, Technical Report, NREL/TP-5500-58274, Golden, CO, May 2013

Eugene Preston and Clayton Barrows. 2018. "Evaluation of Year 2020 IEEE RTS Generation Reliability Indices," 2018 IEEE International Conference on Probabilistic Methods Applied to Power Systems (PMAPS), 24-28 June 2018.

Friedman, J. 2002. Stochastic gradient boosting. Computational Statistics & Data Analysis, 38(4):367–378.

Gillies, R. R., S. Wang, and M. R. Booth. 2010. Atmospheric scale interaction on wintertime Intermountain West low-level inversions. Wea. Forecasting, 25, 1196–1210.

Grenier, H., and C. S. Bretherton. 2001. A moist PBL parameterization for large-scale models and its application to subtropical cloud-topped marine boundary layers. Mon. Wea. Rev., 129, 357-377.

Gultepe, I. 2007. Fog and Boundary Layer Clouds: Fog Visibility and Forecasting, Birkhäuser Basel. http://insidelines.pjm.com/operating-committee-reviews-perfect-dispatch-performance/

Iacono, M.J., J.S. Delamere, E.J. Mlawer, M.W. Shephard, S.A. Clough, W.D. Collins. 2008. Radiative forcing by long - lived greenhouse gases: Calculations with the AER radiative transfer models, Climate and Dynamics, 113: D13103, doi: 10.1029/2008JD009944

ISO New England. 2017. Details on the Use of the Solar Photovoltaic Forecast to Modify the Long-term New England Load Forecast. April 9, 2017.

Janjić, Z, 1994. The step-mountain ETA coordinate model: further development of the convection, viscous sublayer and turbulence closure scheme. Mon Weather Rev 122(5): 927–945

Jimenez, P.A., & Hacker J.P. 2016. WRF-Solar: Description and Clear-Sky Assessment of an Augmented NWP Model for Solar Power Prediction. Bulletin of the American Meteorological Society. https://doi.org/10.1175/BAMS-D-14-00279.1

Kalnay, E., 2002. Atmospheric Modeling, Data Assimilation and Predictability. Cambridge University Press, Cambridge, UK.

Kann A., Schellander-Gorgas T., and Wittmann C. 2015. Enhanced short-range forecasting of sub-inversion cloudiness in complex terrain. Atmos. Sci. Lett. 16(1), 1-9.

Monforte, F,A., Fordham, C., Blanco, J., Barsun, S., Kankiewicz, K., Norris, B. 2016. Improving Short-Term Load Forecasts by Incorporating Solar PV Generation. California Energy Commission. Publication number: CEC-500-2017-031.

Koračin, D., Businger, J. A., Dorman, C. E. and Lewis, J. M. 2005. Formation, Evolution, and Dissipation of Coastal Sea Fog. Boundary-Layer Meteorology 117:3, 447-478, 2014.

Lazard (2019). Levelized Cost of Energy and Levelized Cost of Storage 2019. www.lazard.com/perspective/lcoe2019.

Lundberg, S.M., G.G. Erion, and S.-I. Lee, 2019. Consistent Individualized Feature Attribution for Tree Ensembles, arXiv:1802.03888.

MacDonald C.P., Craig K.J., and Moffet R.C. 2018. Revised sensor deployment plan for the measurements of fog burn-off for improved solar forecasting project. Technical memorandum prepared for the Electric Power Research Institute, Palo Alto, CA, by Sonoma Technology, Inc., Petaluma, CA, STI-917071-6837-TM, January 25.

MacDonald C.P., Craig K.J., Moffet R.C., and Hafner H.R. (2017a) Measurements of fog burn-off for improved solar forecasting: field plan. Prepared for the Electric Power Research Institute, Palo Alto, CA, by Sonoma Technology, Inc., Petaluma, CA, STI-917071-6830, November 30.

MacDonald C.P., Craig K.J., Moffet R.C., and Hafner H.R. (2017b) Measurements of fog burn-off for improved solar forecasting: existing instrumentation use plan. Prepared for the Electric Power Research Institute, Palo Alto, CA, by Sonoma Technology, Inc., Petaluma, CA, STI-917071-6829, December 14.

MacDonald C.P., Craig K.J., Moffet R.C., and Hafner H.R. (2017c) Measurements of fog burn-off for improved solar forecasting: measurement and verification plan. Prepared for the Electric Power Research Institute, Palo Alto, CA, by Sonoma Technology, Inc., Petaluma, CA, STI-917071-6831, November 30.

Marzban C., Leyton S., and Colman B. Ceiling and visibility forecasts via neural networks. Weather and Forecasting, 22(3), 466-479, 2007.

McGovern, A., K.L. Elmore, D.J. Gagne, S.E. Haupt, C.D. Karstens, R. Lagerquist, T. Smith, and J.K. Williams (2017) Using Artificial Intelligence to Improve Real-Time Decision-Making for High-Impact Weather. Bull. Amer. Meteor. Soc., 98, 2073–2090, https://doi.org/10.1175/BAMS-D-16-0123.1.

McGovern, A., R. Lagerquist, D. John Gagne, G.E. Jergensen, K.L. Elmore, C.R. Homeyer, and T. Smith (2019) Making the Black Box More Transparent: Understanding the Physical Implications of Machine Learning. Bull. Amer. Meteor. Soc., 100, 2175–2199, https://doi.org/10.1175/BAMS-D-18-0195.1.

Miller S.D., Rogers M., Haynes J.M., Sengupta M., and Heidinger A.K. (2018) Short-term solar irradiance forecasting via satellite/model coupling. Solar Energy, 168, 102-117, doi: 10.1016/j.solener.2017.11.049

Mills, A. et al. Understanding Variability and Uncertainty of Photovoltaics for Integration with the Electric Power System. Technical Report LBNL-2855E. Berkeley, CA: Lawrence Berkeley National Laboratory, 2009.

Morris V.R. (2006) Microwave radiometer (MWR) handbook. Supported by the U.S. Department of Energy, Office of Science, Office of Biological and Environmental Research, ARM TR-016, August.

N. Kumar et al (2012)., Power Plant Cycling Costs, NREL Tech Report, April 2012. www.nrel.gov/docs/fy12osti/55433.pdf.

NOAA (2019), The High-Resolution Rapid Refresh (HRRR). https://rapidrefresh.noaa.gov/hrrr/.

NREL (2018), GMLC RTS Test System. https://github.com/GridMod/RTS-GMLC.

Price, J. et al. 2011. Reduced network modeling of WECC as a market design prototype, 2011 IEEE Power and Energy Society General Meeting, 24-28 July 2011.

PJM. 2016. https://www.pjm.com/-/media/committees-groups/task-forces/rmistf/20160323/20160323-item-03-update-rto-iso-benchmarking.ashx

Preston, E. and Barrows, C. 2018. Evaluation of Year 2020 IEEE RTS Generation Reliability Indices, 2018 IEEE International Conference on Probabilistic Methods Applied to Power Systems (PMAPS), 24-28 June 2018.

Wang, Q. Hodge, B.M. 2017. Enhancing Power System Operational Flexibility with Flexible Ramping Products: A Review, IEEE Transactions on Industrial Informatics, vol. 13, no. 4, pp. 1652-1664, 2017.

Wang, Q., Brancucci, C., Wu, H., Florita, A.R., Hodge, B.M. 2016a. Quantifying the Economic and Grid Reliability Impacts of Improved Wind Power Forecasting, IEEE Transactions on Sustainable Energy, vol. 7, no. 4, pp. 1525 - 1537, 2016.

Wang,Q., Wu, H., Florita, A.R., Martinez-Anido, C.B., Hodge, B.M. 2016b. The value of improved wind power forecasting: Grid flexibility quantification, ramp capability analysis, and impacts of electricity market operation timescales," Applied Energy, 184, 696-713, 2016.

Skamarock, W. C., et al., 2019. A Description of the Advanced Research WRF Version 4. NCAR Tech. Note NCAR/TN-556+STR, 145 pp, doi:10.5065/1dfh-6p97

Stefferud, K., Schoene, J., Zheglov, V.; Kleissl, J. 2017. Analysis and Modeling of Utility Scale Solar Forecasting. California Energy Commission. Publication number: CEC-500-2017-010.

Wang, Y., S. Gao, G. Fu, J. Sun, and S. Zhang, 2014. Assimilating MTSAT-Derived Humidity in Nowcasting Sea Fog over the Yellow Sea. Wea. Forecasting, 29, 205–225, 2014.

WECC TEPPC. System Adequacy Planning Datasets. https://www.wecc.org/SystemAdequacyPlanning/Pages/Datasets.aspx.

Wilczak J., et al., 2015. The Wind Forecast Improvement Project (WFIP): a public–private partnership addressing wind energy forecast needs. Bulletin of the American Meteorological Society, 96(10), 1699-1718, doi: 10.1175/bams-d-14-00107.1, October 30. Available at https://journals.ametsoc.org/doi/abs/10.1175/BAMS-D-14-00107.1.

Wilczak, J.M., et al., 2019. The Second Wind Forecast Improvement Project (WFIP2): Observational Field Campaign. Bull. Amer. Meteor. Soc., 100, 1701–1723, https://doi.org/10.1175/BAMS-D-18-0035.1.

Wilson, T.H. & Fovell, R.G. 2018. Modeling the Evolution and Life Cycle of Radiative Cold Pools and Fog. Weather and Forecasting. https://doi.org/10.1175/WAF-D-17-0109.1

Wilson, T.H. and R.G. Fovell. 2018. Modeling the Evolution and Life Cycle of Radiative Cold Pools and Fog. Weather and Forecasting, 33:203-220, doi: 10.1175/WAF-D-17-0109.1

WRF Model Physics Options & References. 2020. University Corporation for Atmospheric Research (UCAR) Website. Available at http://www2.mmm.ucar.edu/wrf/users/phys_references.html

Xie, Y., Sengupta, M., Dudhia, J. 2016. A Fast All-sky Radiation Model for Solar applications (FARMS): Algorithm and performance evaluation. Solar Energy 135, 435–445.

Zack J.W. and Craig K.J. 2017. Measurements of fog burn-off for improved solar forecasting: forecast specifications document. Prepared for the Electric Power Research Institute, Palo Alto, CA, by AWS Trupower, Albany, NY, and Sonoma Technology, Inc., Petaluma, CA, STI-917071-6835, December 15.

Zhang, J., Florita, A., Hodge, B.M., Lu, S., Hamann, H.F., Banunarayanan, V., Brockway, A. 2015. A suite of metrics for assessing the performance of solar power forecasting, Solar Energy, Volume 111, January 2015, Pages 157-175.